NASA TECHNICAL NOTE

NASA TN D-2543

NASA TN D-2543

EFFECT OF ENVIRONMENTAL PARAMETERS ON THE PERFORMANCE OF LOW-DENSITY SILICONE-RESIN AND PHENOLIC-NYLON ABLATION MATERIALS

by Ronald K. Clark

Langley Research Center
Langley Station, Hampton, Va.

NATIONAL AERONAUTICS AND SPACE ADMINISTRATION • WASHINGTON, D. C. • JANUARY 1965

EFFECT OF ENVIRONMENTAL PARAMETERS ON THE PERFORMANCE OF LOW-DENSITY SILICONE-RESIN AND PHENOLIC-NYLON ABLATION MATERIALS

By Ronald K. Clark

Langley Research Center
Langley Station, Hampton, Va.

NATIONAL AERONAUTICS AND SPACE ADMINISTRATION

For sale by the Office of Technical Services, Department of Commerce,
Washington, D.C. 20230 -- Price $2.00

EFFECT OF ENVIRONMENTAL PARAMETERS ON THE PERFORMANCE OF LOW-DENSITY SILICONE-RESIN AND PHENOLIC-NYLON ABLATION MATERIALS

By Ronald K. Clark
Langley Research Center

SUMMARY

Thermal performance data were obtained for low-density phenolic-nylon and low-density silicone resin in the 2500-kilowatt arc jet at the Langley Research Center over a range of heating rates from 10 to 242 Btu/ft^2-sec (0.113 to 2.75 MW/m^2) and a range of aerodynamic shear stresses from 0 to 7.2 lb/ft^2 (0 to 344 N/m^2) at jet-stream oxygen concentrations ranging from 0 to 23 percent. With use of these data, analyses were made of the relative effect of environmental parameters such as heating rate, free-stream oxygen concentration, stagnation enthalpy, and aerodynamic shear stress on the performance of these materials.

Principal conclusions resulting from this study include (1) In a low-oxygen-content stream of the 2500-kilowatt jet, the performance of low-density silicone resin is superior to that of low-density phenolic-nylon at heating rates ranging from 80 to 150 Btu/ft^2-sec (0.91 to 1.70 MW/m^2) and at shear stresses near 4.7 lb/ft^2 (225 N/m^2); however, at heating rates outside this range, low-density phenolic-nylon is superior to low-density silicone resin. (2) Low-density silicone resin is highly sensitive to the combined effects of surface temperature and aerodynamic shear; thus, a drastic reduction in performance occurs for heating rates above 150 Btu/ft^2-sec (1.70 MW/m^2). However, increasing the heating rate up to 242 Btu/ft^2-sec (2.75 MW/m^2) and the shear stress up to 7.2 lb/ft^2 (344 N/m^2), which was the most severe condition obtained, resulted in a continuing increase in the performance of phenolic-nylon. (3) Low-density phenolic-nylon is highly sensitive to oxygen in the jet stream at all heating rates investigated, whereas low-density silicone resin is not affected by this factor except, possibly, at heating rates above 150 Btu/ft^2-sec (1.70 MW/m^2).

INTRODUCTION

The Langley Research Center has a continuing program to evaluate the effectiveness of prospective reentry heat-shield materials. The initial step in the evaluation of such materials consists of subjecting them to a standard

screening test. Under this test a material is investigated at convective heating rates ranging from 100 to 110 Btu/ft^2-sec (1.13 to 1.25 MW/m^2) in an air environment until a specified back-surface temperature is reached. The time required for a material to reach the specified temperature is used as a measure of its thermal effectiveness. Based on the resulting data, the materials providing the higher values of thermal effectiveness are selected for further investigation.

Recent data obtained in a screening program indicated that a low-density silicone resin supported by a honeycomb core has a superior performance. The residue of this type of material is primarily siliceous; hence, it is not as prone to oxidation as those materials which form carbonaceous chars. An engineering analysis of the simulation of flight oxidation conditions in ground facilities, which was made at the Langley Research Center, has indicated that low-enthalpy air environments, such as were used in the screening tests, cause more oxidation than flight conditions. This greater oxidation results from the fact that low-enthalpy facilities require a much higher mass flow rate to give a certain heating rate than is encountered on reentry to the earth's atmosphere. Under screening test conditions, materials with siliceous residues appear to be superior to those with carbonaceous residues, which are more susceptible to oxidation. However, this may not be the case in an environment more nearly simulating the flight environment. Since a melt phase is present with the siliceous residue, the performance of this material might be adversely affected by other conditions of heating rate, enthalpy, and aerodynamic shear.

The project reported herein was undertaken to investigate the relative effects of such environmental parameters as free-stream oxygen concentration, stagnation enthalpy, aerodynamic shear, and cold-wall heat-transfer rate on the performance of low-density elastomeric ablators and low-density charring composite ablators. The materials investigated were a low-density silicone resin and a low-density phenolic-nylon material.

Low-density phenolic-nylon was chosen as the reference material with which to compare low-density silicone resin. It was selected as being representative of low-density carbonaceous charring ablators.

SYMBOLS

The units used for the physical quantities defined in this section are given in both the U.S. customary units and in the International System of Units (SI). (See ref. 1.) Appendix A is included for the purpose of explaining the relationships between these two systems of units.

A area, ft^2 (m^2)

C free-stream oxygen concentration, percent

C_F skin-friction coefficient

c_p specific heat at constant pressure, Btu/lb-^oR (J/kg-^oK)

E effectiveness of ablation material, $\frac{\dot{q}t}{w}$, Btu/lb (J/kg)

H enthalpy, Btu/lb (J/kg)

h coefficient of heat transfer, Btu/ft^2-sec-^oR (W/m^2-^oK)

$\dot{m}(O_2)$ oxygen mass transfer through boundary layer to surface, $\frac{C\dot{q}}{(H_\infty - H_w)}$, lb/ft^2-sec (kg/m^2-s)

N_{Pr} Prandtl number, $\frac{c_p\mu}{k}$

N_{St} Stanton number, $\frac{h}{c_p\rho V}$

p_d dynamic pressure, lb/ft^2 (N/m^2)

$\dot{q}$ cold-wall heat-transfer rate, Btu/ft^2-sec (W/m^2)

T temperature, ^oF (^oK)

t time, sec (s)

V velocity, ft/sec (m/s)

$\dot{W}$ mass flow, lb/sec (kg/s)

w specimen weight per unit area, lb/ft^2 (kg/m^2)

ρ density, lb/ft^3 (kg/m^3)

μ viscosity, lb/ft-sec (N-s/m^2)

τ aerodynamic shear stress, lb/ft^2 (N/m^2)

Subscripts:

av average

e experimental

p predicted

w wall

∞	free stream
300	state when back-surface temperature rise equals 300° F (167° K)

TEST FACILITY AND MATERIALS

Test Facility

The results reported in this paper were obtained in the 2500-kilowatt arc jet at the Langley Research Center. For this investigation, a subsonic nozzle was fitted to the jet, which is shown in figure 1 and described in reference 2. This facility has provisions for varying the mass flow per unit area, chemical composition of the test stream, and power input to the arc electrodes. The stream enthalpy is controlled by varying the power input to the electrodes and/or the stream mass flow.

Materials

The materials evaluated were a honeycomb-supported low-density silicone resin and a low-density phenolic-nylon. The density of the silicone resin was 55 lb/ft^3 (880 kg/m^3). The honeycomb support in the silicone resin had 3/16-inch (4.76-mm) hexagonal cells and was made from a phenolic-glass material. The low-density phenolic-nylon, which has a density of about 36 lb/ft^3 (576 kg/mg^3), has the following composition by weight:

(a) 23-percent phenolic resin

(b) 47-percent nylon

(c) 25-percent hollow phenolic microspheres

(d) 5-percent hollow silica microspheres

These materials were fabricated into specimens 3 inches in diameter and of such thickness that their weights per unit area were 3 lb/ft^2 (14.7 kg/m^2). Each specimen was bonded to a brass support ring. A copper calorimeter, which has a thickness of 1/8 inch (0.32 cm) and a diameter of 1/2 inch (1.27 cm) and is surrounded by a copper guard ring having a thickness of 1/8 inch (0.32 cm), was attached to the back surface as illustrated in figure 2. Two thermocouples were attached to the calorimeter to monitor the back-surface temperature.

TEST CONDITIONS AND PROCEDURE

Test Conditions

Test variables included oxygen concentration, enthalpy, mass flow per unit area, power input to the arc jet, shear stress on the specimen surface, and

cold-wall heat-transfer rate. Controlled variables were rate of cold-wall heat transfer to the specimen, which was varied from 10 to 242 Btu/ft^2-sec (0.113 to 2.75 MW/m^2), and oxygen concentration of the test stream, which was varied from 0 to 23 percent. Changes in the heat-transfer rate were effected by regulating the test-stream mass flow rate and enthalpy and the power input to the arc jet. The mass flow rate ranged from 0.2 to 16 lb/ft^2-sec (0.97 to 78 kg/m^2-sec); enthalpy, 1675 to 4000 Btu/lb (3.88 to 9.28 MJ/kg); and shear stress, 0 to 7.2 lb/ft^2 (0 to 344 N/m^2).

Test Procedure

In order to obtain a given heating rate, the mass flow per unit area was selected so that heating rates near the desired value would result; then, by adjusting the electrical power input to the jet, the heating rate was adjusted to the desired value. Changing the power input results in changes in the test-stream enthalpy. Heat-transfer rate was measured by a continuous-acting 3/8-inch-diameter (0.953-cm) calorimeter (described in ref. 2), which had previously been calibrated by a calorimeter with the same geometry as that of the specimens tested.

Oxygen content of the test stream was controlled by regulating the relative amounts of nitrogen and air entering the arc chamber of the jet. Tests were conducted for oxygen concentrations of 0, 3, 11, and 23 percent. An analysis made at the Langley Research Center indicates that the effects on the test specimen in the 2500-kilowatt jet stream with a reduced oxygen content more nearly simulate reentry char oxidation than do the effects in a jet stream with a greater oxygen content; hence, more tests were conducted at an oxygen concentration of 3 percent than at other concentrations. This result was established from the fact that simulation of char-layer oxidation is accomplished by adjusting the test-stream oxygen content to equal the product of flight oxygen content and the ratio of test-stream enthalpy to flight enthalpy.

The shear stresses acting on the exposed surfaces were calculated from a theoretical relationship presented in appendix B. These values of shear stress are reference values and are not to be taken as absolute.

Values of stream enthalpy were obtained from calibration data for the 2500-kilowatt arc jet. These calibration enthalpies were obtained from the free-stream temperature, which was measured by the atomic-line intensity-ratio method by using the electronic excitation spectrum of copper that appears in the gas from the small contamination caused by the electrodes. This method of gas temperature measurement is discussed in reference 3. A simple medium glass spectrograph was used in conjunction with a photoelectric readout system for recording the intensity ratio of the copper lines at 5153 Å and 5700 Å. By assuming thermodynamic equilibrium, the temperature becomes a function of this intensity ratio.

Data recorded during these tests include specimen back-surface temperature history, cold-wall heating rate, still photographs of the specimen after

exposure, and motion pictures of the specimen during exposure. Both the back-surface temperature and the heating rate were recorded on an oscillograph. Still photographs of the specimens after exposure were obtained with a 70-millimeter camera. Motion pictures of the tests were provided through use of a 16-millimeter camera with color film.

Each of the specimens for this project was exposed to the test stream until the oscillograph indicated a back-surface temperature rise of 300° F (167° K).

RESULTS AND DISCUSSION

Tables I and II present summaries of the test conditions and results for the low-density phenolic-nylon and low-density silicone resin, respectively.

Figure 3 presents back-surface temperature histories for low-density phenolic-nylon and low-density silicone resin investigated in air and nitrogen at the maximum and minimum heating rates obtained. Note the large decrease in exposure time for both materials in air at the high heating rate as compared with the time for the same materials in nitrogen.

The performance of these materials was judged by the general appearance of the specimens after exposure to the test stream and by a performance factor known as the effectiveness and defined as

$$E = \dot{q}t/w$$

Low-Density Phenolic-Nylon

Figure 4 presents data obtained for phenolic-nylon for a range of heating rates from 82 to 242 Btu/ft^2-sec (0.93 to 2.75 MW/m^2). This figure illustrates the dependence of effectiveness upon heating rate and oxygen concentration. The effectiveness increases with heating rate and decreases with increases in oxygen concentration at a given heating rate. The effect of increasing the rate of heat transfer to a phenolic-nylon ablative surface exposed to a stream with a low oxygen content is an increase in the temperature of the exposed surface and, thus, an increase in the quantity of heat radiated from the surface. The heating rate was increased at a given mass flow rate by elevating the stream enthalpy, which increases the energy blockage effect of pyrolysis gases flowing through the char into the boundary layer. The combined results of the increased radiation of energy by the surface and the greater amounts of energy blocked by the pyrolysis gases entering the boundary layer as the rate of heat transfer to the specimen is increased account for the increase in effectiveness with heating rate shown in figures 4 and 5.

Oxygen in the test stream results in oxidation of the char layer, which serves as a shield for the uncharred material. This combustion of the char layer results in an additional transfer of energy to the ablator (ref. 4); thus, its effectiveness at a given cold-wall heat-transfer rate is reduced. Char

loss due to oxidation in streams of low oxygen content is a diffusion-controlled process whereby all oxygen reaching the char surface is consumed by the chemical process of oxidation. Under this condition an increase in the stream oxygen content results in a similar increase in the char oxidation rate. In streams of higher oxygen content the system nears saturation with oxygen and the char loss rate due to oxidation is a reaction-rate-controlled process, the rate of which is highly dependent upon the char surface temperature.

As indicated previously, more investigations were made with oxygen concentrations of 3 percent than with other concentrations. Figure 5 gives the results of these investigations for low-density phenolic-nylon. It should be reiterated that a specific heating rate is obtained for a given mass flow by altering the power input to the jet. Such changes in the power input result in changes in the enthalpy of the jet stream. Hence, the combined effects of heating rate, enthalpy, aerodynamic shear, and oxidation are presented in figure 5.

In an effort to correlate a relationship between the variables of effectiveness, heating rate, free-stream enthalpy, aerodynamic shear stress, and oxidation as related to low-density phenolic-nylon, a multiple linear regression analysis was made by using the data obtained for phenolic-nylon.

Briefly, a multiple linear regression analysis consists of assuming a relationship between the parameters of concern. For this case the assumed relationship between the parameters is

$$E_p = aH + b\dot{q} + c\dot{m}(O_2) + d\tau + e \tag{1}$$

where a, b, c, d, and e are coefficients to be determined. The error in this assumption is given by

$$\Delta = E_e - E_p = E_e - \left(aH + b\dot{q} + c\dot{m}(O_2) + d\tau + e\right) \tag{2}$$

Squaring Δ, summing over all data points, and differentiating partially with respect to the coefficient a gives

$$\frac{\partial}{\partial a}\sum \Delta^2 = \sum\left[\frac{\partial}{\partial a}\left(E_e - aH - b\dot{q} - c\dot{m}(O_2) - d\tau - e\right)^2\right]$$

$$= -2\left(\sum HE_e - a\sum H^2 - b\sum \dot{q}H - c\sum \dot{m}(O_2)H - d\sum \tau H - e\sum H\right) \tag{3}$$

Setting this derivative equal to zero gives the minimum sum of squared errors; thus,

$$\sum HE_e = a\sum H^2 + b\sum \dot{q}H + c\sum \dot{m}(O_2)H + d\sum \tau H + e\sum H \tag{4}$$

Similarly, taking the partial derivatives with respect to b, c, d, and e and setting each result equal to zero yields four more equations. Solving these five equations for a, b, c, d, and e and substituting into equation (1) gives

$$E_p = 0.92H + 47\dot{q} - 564{,}000\dot{m}(O_2) - 378\tau + 5740 \qquad (5)$$

Equation (5) indicates an increase in predicted effectiveness with any increase in stream enthalpy or heating rate and a decrease in predicted effectiveness with any increase in oxygen mass transfer to the material surface or aerodynamic shear stress. In order to interpret this equation, some knowledge of the magnitude of each variable term to the right of the equal sign relative to the constant 5740 Btu/lb (13.3 MJ/kg) must be known.

The ranges of the environmental variables for phenolic-nylon, which are given in table I, are: enthalpy, 1675 to 4000 Btu/lb (3.89 to 9.28 MJ/kg); heating rate, 39 to 242 Btu/ft^2-sec (0.44 to 2.75 MW/m^2); oxygen mass transfer to the material surface, 0 to 0.0155 lb/ft^2-sec (0 to 0.075 kg/m^2-s); and aerodynamic shear stress, 0 to 7.2 lb/ft^2 (0 to 344 N/m^2). These ranges give variable-term ranges of: enthalpy term, 1540 to 3680 Btu/lb (3.57 to 8.53 MJ/kg); heating-rate term, 1830 to 11,380 Btu/lb (4.25 to 26.4 MJ/kg); oxygen-mass-transfer term, 0 to -8590 Btu/lb (0 to -19.9 MJ/kg); and aerodynamic-shear-stress term, 0 to -2720 Btu/lb (0 to -6.30 MJ/kg). A comparison of these numbers with each other and with the constant 5740 Btu/lb (13.3 MJ/kg) indicates that low-density phenolic-nylon is far less sensitive to the effects of aerodynamic shear stress than to the effects of oxidation - in each case these effects are negative. Both test-stream enthalpy and heating rate have positive effects on the effectiveness of low-density phenolic-nylon; however, heating rate is a much more significant factor than enthalpy.

Figures 6 to 11 are photographs of the low-density phenolic-nylon specimens. Points observed from viewing motion pictures, taken during the investigations, and specimen remains include (1) Investigations in nitrogen at high total mass flow rates showed no erosion of the specimen surface; whereas, with some oxygen in the test stream, varying degrees of spalling and apparent flowing and bubbling of the exposed surface occurred, depending upon the amount of oxygen present. Thus, a more pitted and rougher surface resulted in test streams containing some oxygen than in nonoxidizing environments. (Figs. 6 and 7 show some decrease in specimen dimensions for investigations in nitrogen, but this decrease is attributed to shrinkage of the char after pyrolysis.) (2) Large variations in oxygen mass flow per unit area result in appreciable changes in stagnation-point recession and char thickness.

It is believed that the apparent flowing and bubbling of the exposed phenolic-nylon surfaces was actually glowing bubbles of oxidation and pyrolysis products (some of which may still be undergoing chemical reactions) entering the stream from the specimen surface. Severe oxidation results in rough, pitted, and structurally weak surfaces which are more susceptible to spalling. The observations enumerated in the previous paragraph together with the results from the regression analysis indicate that shear levels of the magnitude experienced do not severely affect the behavior of low-density phenolic-nylon.

Figure 12 shows the effectiveness of phenolic-nylon as a function of oxygen concentration for a constant heating rate of 120 Btu/ft^2-sec (1.36 MW/m^2) at values of mass flow per unit area of 4 and 16 lb/ft^2-sec (19.4 and 78 kg/m^2-sec), which result in radically different values of enthalpy, shear, and oxygen mass flow per unit area. These plots were obtained by cross-plotting data from plots of the effectiveness as a function of heating rate. It was shown previously that the effects of shear are not severe for this investigation; hence, the difference in effectiveness for the two mass flows at a given oxygen concentration results primarily from the combined effects of the different values of enthalpy and oxygen mass transfer to the specimen surface. These effects seem to be similar throughout the range of oxygen concentrations as evidenced by the near parallelism of the two curves. The higher enthalpy and lower oxygen-mass-transfer rate for the upper curve are more conducive to high performance than are the conditions for the lower curve. Note the large difference in effectiveness even at an oxygen concentration of 23 percent; this difference results from the greater protection provided by the thicker char layer at a mass flow per unit area of 4 lb/ft^2-sec (19.4 kg/m^2-sec) and the larger amounts of heat blocked by pyrolysis gases entering the boundary layer as discussed previously.

It is significant that low-density phenolic-nylon suffers a greater loss in effectiveness with increases in oxygen content of the stream at concentrations below 10 percent than at values above 10 percent. For streams with low oxygen content, oxidation of the char surface occurs at such a rate that no surplus oxygen is present; hence, an increase in oxygen content results in a similar increase in char oxidation. However, as the oxygen content increases the system approaches a point where a surplus of oxygen is present and the oxidation rate depends on the temperature of the char surface.

Low-Density Silicone Resin

Effectiveness plots for low-density silicone resin are presented in figure 13 for four oxygen concentrations ranging from 0 to 23 percent. The most obvious feature shown is the high degree of conformity in performance for all stream compositions at heating rates less than 150 Btu/ft^2-sec (1.70 MW/m^2). This conformity is to be expected since maximum chemical and thermal shielding of the char layer is obtained from the molten glass layer which is quite viscous at temperatures in this heating-rate range. Another significant point illustrated in figure 13 is the sharp drop in effectiveness for heating rates above 150 Btu/ft^2-sec (1.70 MW/m^2). This decrease in performance results from loss of shielding caused by flow-off of the molten glass at high temperatures and shear stresses. There is no evidence that oxygen concentration affects the performance of low-density silicone resin except, possibly, for heating rates above 150 Btu/ft^2-sec (1.70 MW/m^2), and this variation of performance could be due to scatter in the data.

Motion pictures taken during the investigation of the low-density silicone resin indicate that the shear levels obtained at high total-mass-flow and heating rates were sufficient to cause the low-viscosity molten glass layer to flow away from the stagnation region leaving it unshielded from the test stream.

This behavior is illustrated in figure 14, which shows that the siliceous layer covering the surface is very thin; also evident is the layer which melted and flowed to the outer edge of the specimen during exposure.

Figures 15 to 17 present photographs representative of the silicone-resin specimens investigated. It is evident from an examination of the remains after exposure at a high heating rate and a high shear stress in nitrogen (fig. 15) and in oxidizing environments, where there was essentially no material remaining to photograph, that low-density silicone resin is sensitive to the combined effects of shear and oxidation. Figures 16 and 17 show little effects of shear or oxidation; in fact, because of swelling of the material when heated, all specimens were thicker after exposure, except those subjected to a high heating rate in a high-mass-flow stream.

The surface of silicone-resin specimens is covered with a siliceous layer after exposure. The thickness of this layer is dependent upon the surface temperature and the shear stress acting on the specimen during exposure. As shown in figures 15 to 17 there is no tendency for silicone resin to lose its char; in fact, the remains of these specimens are quite rugged.

Figure 18 summarizes the results for low-density phenolic-nylon and low-density silicone resin investigated in a stream with an oxygen concentration of 3 percent. Note that the performance of silicone resin is superior to that of phenolic-nylon for heating rates in the range of 80 to 150 Btu/ft^2-sec (0.91 to 1.70 MW/m^2) and for shear stresses near 4.7 lb/ft^2 (225 N/m^2), whereas phenolic-nylon is the better performer under other conditions investigated.

CONCLUSIONS

An investigation of the effect of some environmental parameters on the relative performance of low-density silicone resin and low-density phenolic-nylon made in the 2500-kilowatt arc jet at the Langley Research Center has resulted in the following conclusions:

1. In the 2500-kilowatt jet stream of low oxygen content, the performance of low-density silicone resin is superior to that of low-density phenolic-nylon at heating rates ranging from 80 to 150 Btu/ft^2-sec (0.91 to 1.70 MW/m^2) and at shear stresses near 4.7 lb/ft^2 (225 N/m^2); however, phenolic-nylon is superior to silicone resin in a low-oxygen-content stream at heating rates outside this range.

2. Low-density silicone resin is highly sensitive to the combined effects of surface temperature and aerodynamic shear; thus, a drastic reduction in performance occurs for heating rates above 150 Btu/ft^2-sec (1.70 MW/m^2). However, increasing the heating rate up to 242 Btu/ft^2-sec (2.75 MW/m^2) and the shear stress up to 7.2 lb/ft^2 (344 N/m^2), which was the most severe condition obtained, resulted in a continuing increase in the performance of phenolic-nylon.

3. Low-density phenolic-nylon is highly sensitive to oxygen in the jet stream at all heating rates investigated, whereas low-density silicone resin is not affected by this factor except, possibly, at heating rates above 150 Btu/ft^2-sec (1.70 MW/m^2).

Langley Research Center,
National Aeronautics and Space Administration,
Langley Station, Hampton, Va., September 3, 1964.

APPENDIX A

CONVERSION OF U.S. CUSTOMARY UNITS TO SI UNITS

The International System of Units, abbreviated SI (Systeme International), was adopted in 1960 by the Eleventh General Conference on Weights and Measures held in Paris, France. Conversion factors required for units used herein are given in the following table:

Physical quantity	U.S. customary unit	Conversion factor (*)	SI unit
Aerodynamic shear stress	lb/ft^2	47.88	N/m^2
Coefficient of heat transfer	$Btu/ft^2\text{-sec-}^oR$	2.04×10^4	$W/m^2\text{-}^oK$
Density	lb/ft^3	16.02	kg/m^3
Dynamic pressure	lb/ft^2	47.88	N/m^2
Enthalpy	Btu/lb	2.32×10^3	J/kg
Heat-transfer rate	$Btu/ft^2\text{-sec}$	1.135×10^4	W/m^2
Length	ft	0.3048	m
	in.	0.0254	m
Mass distribution	lb/ft^2	4.88	kg/m^2
Mass flow per unit area	$lb/ft^2\text{-sec}$	4.85	$kg/m^2\text{-s}$
Specific heat	$Btu/lb\text{-}^oR$	4.18×10^3	$J/kg\text{-}^oK$
Temperature	^oF	$\frac{5}{9}(^oF + 460)$	^oK
Temperature rise	^oF	0.556	^oK
Thermal effectiveness	Btu/lb	2.32×10^3	J/kg
Velocity	ft/sec	0.305	m/s

*Multiply value given in U.S. customary unit by conversion factor to obtain equivalent value in SI unit.

Prefixes to indicate multiples of units are:

Prefix	Multiple
mega (M)	10^6
centi (c)	10^{-2}
milli (m)	10^{-3}

APPENDIX B

COMPUTATION OF SHEAR FORCES ON A FLAT-FACED SPECIMEN EXPOSED TO A HIGH-ENERGY STREAM

Heat flow through the boundary layer is given by the Fourier equation as

$$\dot{q} = h(T_\infty - T_w) \tag{B1}$$

Shear stress is given by

$$\tau = C_F p_d \tag{B2}$$

The Stanton number is defined as (ref. 5)

$$N_{St} = \frac{C_F}{2(N_{Pr})^{2/3}} = \frac{h}{c_{p,\infty}\rho_\infty V_\infty} \tag{B3}$$

From equations (1), (2), and (3)

$$\tau = \frac{2p_d(N_{Pr})^{2/3}\dot{q}}{c_{p,\infty}\rho_\infty V_\infty(T_\infty - T_w)} \tag{B4}$$

However,

$$c_{p,\infty}(T_\infty - T_w) = H_\infty - H_w \tag{B5}$$

and

$$\rho_\infty V_\infty = \frac{\dot{W}}{A} \tag{B6}$$

Therefore,

$$\tau = \frac{2(N_{Pr})^{2/3} p_d \dot{q}}{(\dot{W}/A)(H_\infty - H_w)} \tag{B7}$$

The Prandtl number is assumed to be constant and equal to 0.7 for the range of conditions investigated; hence

$$\tau = \frac{1.576 p_d \dot{q}}{(\dot{W}/A)(H_\infty - H_w)} \tag{B8}$$

Values of shear stress obtained from this equation are considered representative of the maximum levels of shear acting on the specimens at the outer edge.

REFERENCES

1. Anon.: International System of Units, Resolution No. 12. NASA TT F-200, 1964.

2. Chapman, Andrew J.: An Experimental Evaluation of Three Types of Thermal Protection Materials at Moderate Heating Rates and High Total Heat Loads. NASA TN D-1814, 1963.

3. Pearce, Willard J.: Plasma Jet Temperature Study. WADC Tech. Rep. 59-346, U.S. Air Force, Feb. 1960.

4. Dow, Marvin B.; and Swann, Robert T.: Determination of Effects of Oxidation on Performance of Charring Ablators. NASA TR R-196, 1964.

5. Dorrance, William H.: Viscous Hypersonic Flow. McGraw-Hill Book Co., Inc., c.1962.

TABLE I.- SUMMARY OF RESULTS FOR LOW-DENSITY PHENOLIC-NYLON

(a) U.S. customary units

[ρ = 36 lb/ft3; w = 3 lb/ft2; specimen thickness = 1.0 inch]

Specimen	Stream diam, in.	$\dot{W}/A$, $\frac{lb}{ft^2\text{-sec}}$	C, percent	$\dot{q}$, Btu/ft^2-sec	H_∞, Btu/lb	τ, lb/ft^2	$\dot{m}(O_2)$, lb/ft^2-sec	t_{300}, sec	E_{300}, Btu/lb	Wt. loss, percent	Thickness, in.		
											Total	Virgin	Char
1	2	16	23	140	2200	5.91	0.0155	141	6560	(a)	(a)	(a)	(a)
2	2	16	23	206	3650	6.60	.0135	101	6950	92	0.15	0.12	0.03
3	2	16	11	107	2100	4.54	.0060	202	7200	(a)	.19	(a)	(a)
4	2	16	11	200	3500	6.43	.0065	140	9320	(a)	.19	.09	.10
5	2	16	3	100	2025	4.12	.0016	234	7800	95	.15	.12	.03
6	2	16	3	128	2150	5.38	.0019	234	9984	94	.34	.29	.05
7	2	16	3	170	2950	6.20	.0018	241	13660	(a)	.20	.07	.13
8	2	16	3	201	3500	6.46	.0018	200	13400	94	.20	(a)	(a)
9	2	16	3	205	3625	6.52	.0018	229	15645	98	.29	.12	.17
10	2	16	3	207	3650	6.60	.0018	193	13300	95	.20	.02	.18
11	2	16	3	242	4000	7.20	.0019	207	16700	96	.09	.02	.07
12	2	16	0	82	2000	3.41	0	376	10280	79	.87	.02	.85
13	2	16	0	198	3550	6.35	0	292	19280	68	.75	.05	.70
14	4	4	23	78	2100	.76	.0091	282	7340	(a)	.25	.04	.21
15	4	4	23	120	3550	.95	.0081	222	8870	(a)	.20	(a)	(a)
16	4	4	11	49	1800	.52	.0032	388	5850	85	.50	.29	.21
17	4	4	11	50	1800	.52	.0033	382	6350	88	.43	.24	.19
18	4	4	11	102	3250	.84	.0036	280	9580	89	.37	.09	.28
19	4	4	3	50	1675	.55	.0010	471	7840	76	.78	.30	.48
20	4	4	3	78	2400	.72	.0010	427	11100	84	.68	.18	.50
21	4	4	3	103	3050	.87	.0011	364	12500	77	.78	.22	.56
22	4	4	3	130	3575	1.02	.0011	314	13600	71	.83	.21	.62
23	4	4	0	49	1800	.52	0	594	9700	64	.97	.14	.83
24	4	4	0	108	3300	.88	0	449	16180	65	.97	.02	.95
25	6	1.8	23	66	2350	.27	.0068	363	7990	(a)	.48	.17	.31
26	6	1.8	23	104	3750	.38	.0066	281	9730	96	.32	(a)	(a)
27	6	1.8	11	42	1750	.20	.0028	569	7970	83	.42	(a)	(a)
28	6	1.8	11	66	2250	.27	.0034	445	9790	74	.72	.24	.48
29	6	1.8	11	68	2350	.27	.0034	406	9200	72	.77	.36	.41
30	6	1.8	3	43	1750	.20	.0008	573	8210	78	.77	.28	.49
31	6	1.8	3	66	2250	.27	.0009	497	10920	61	.85	.43	.42
32	6	1.8	3	80	3050	.30	.0008	453	12100	77	.87	(a)	(a)
33	6	1.8	0	39	1825	.18	0	797	10350	66	.90	.03	.87
34	6	1.8	0	43	2250	.20	0	786	11250	74	.80	(a)	(a)
35	6	1.8	0	97	3650	.34	0	461	15000	73	.80	(a)	(a)
36	12	.2	23	20	(b)	0	(b)	934	6224	78	.72	.59	.13
37	12	.2	0	10	(b)	0	0	1260	(c)	47	.94	.60	.34

[a]Specimen damaged before postexposure data taken.

[b]No spectrographic data available for 12-inch test stream.

[c]Test ended after 1260 seconds (ΔT = 241° F (134° K)).

TABLE I.- SUMMARY OF RESULTS FOR LOW-DENSITY PHENOLIC-NYLON - Concluded

(b) SI units

[ρ = 576 kg/m^3; w = 14.7 kg/m^2; specimen thickness = 2.54 cm]

Specimen	Stream diam, cm	$\dot{W}/A$, kg/m^2-sec	C, percent	$\dot{q}$, MW/m^2	H_∞, MJ/kg	τ, N/m^2	$\dot{m}(O_2)$, kg/m^2-s	t_{300}, s	E_{300}, MJ/kg	Wt. loss, percent	Thickness, mm		
											Total	Virgin	Char
1	5.08	78	23	1.59	5.10	283	0.075	141	15.2	(a)	(a)	(a)	(a)
2	5.08	78	23	2.34	8.47	316	.066	101	16.1	92	3.81	3.05	0.76
3	5.08	78	11	1.21	4.87	217	.029	202	16.7	(a)	4.83	(a)	(a)
4	5.08	78	11	2.27	8.12	308	.032	140	21.6	(a)	4.83	2.29	2.54
5	5.08	78	3	1.13	4.70	197	.008	234	18.1	95	3.81	3.05	.76
6	5.08	78	3	1.45	4.98	258	.009	234	23.2	94	8.6	7.36	1.27
7	5.08	78	3	1.93	6.84	297	.009	241	31.7	(a)	5.1	1.78	3.3
8	5.08	78	3	2.28	8.12	310	.009	200	31.1	94	5.1	(a)	(a)
9	5.08	78	3	2.33	8.41	312	.009	229	36.3	98	7.4	3.05	4.32
10	5.08	78	3	2.35	8.47	316	.009	193	30.9	95	5.1	.51	4.57
11	5.08	78	3	2.75	9.28	344	.009	207	38.7	96	2.29	.51	1.78
12	5.08	78	0	.93	4.64	163	0	376	23.8	79	22.1	.51	21.6
13	5.08	78	0	2.25	8.24	304	0	292	44.7	68	20.1	14.7	5.33
14	10.16	19.4	23	.89	4.87	36.4	.044	282	17.0	(a)	6.35	1.02	5.33
15	10.16	19.4	23	1.36	8.24	45.5	.039	222	20.6	(a)	5.1	(a)	(a)
16	10.16	19.4	11	.56	4.17	24.9	.016	388	13.6	85	12.7	7.37	5.33
17	10.16	19.4	11	.57	4.17	24.9	.016	382	14.7	88	10.9	6.1	4.83
18	10.16	19.4	11	1.16	7.54	40.2	.017	280	22.2	89	9.4	2.29	7.1
19	10.16	19.4	3	.57	3.89	26.3	.005	471	18.2	76	19.8	7.62	12.2
20	10.16	19.4	3	.89	5.57	34.5	.005	427	25.8	84	17.3	4.57	12.7
21	10.16	19.4	3	1.17	7.08	41.7	.005	364	29.0	77	19.8	5.59	14.2
22	10.16	19.4	3	1.48	8.29	48.8	.005	314	31.6	71	21.1	5.33	15.7
23	10.16	19.4	0	.56	4.17	24.9	0	594	22.5	64	24.6	3.56	21.1
24	10.16	19.4	0	1.23	7.65	42.1	0	449	37.5	65	24.6	.51	24.1
25	15.24	8.7	23	.75	5.45	12.9	.033	363	18.5	(a)	12.2	4.32	7.87
26	15.24	8.7	23	1.18	8.70	18.2	.032	281	22.6	96	8.1	(a)	(a)
27	15.24	8.7	11	.48	4.06	9.6	.014	569	18.5	83	10.7	(a)	(a)
28	15.24	8.7	11	.75	5.22	12.9	.016	445	22.7	74	18.3	6.1	12.2
29	15.24	8.7	11	.77	5.45	12.9	.016	406	21.3	72	19.5	9.14	10.4
30	15.24	8.7	3	.49	4.06	9.6	.004	573	19.0	78	19.5	7.11	12.4
31	15.24	8.7	3	.75	5.22	12.9	.004	497	25.3	61	21.6	10.92	10.7
32	15.24	8.7	3	.91	7.08	14.4	.004	453	28.1	77	22.1	(a)	(a)
33	15.24	8.7	0	.44	4.23	8.6	0	797	24.0	66	22.9	.76	22.1
34	15.24	8.7	0	.49	5.22	9.6	0	786	26.1	74	20.3	(a)	(a)
35	15.24	8.7	0	1.1	8.47	16.3	0	461	34.8	73	20.3	(a)	(a)
36	30.48	.97	23	.227	(b)	0	(b)	934	14.4	78	18.3	15	3.3
37	30.48	.97	0	.113	(b)	0	0	1260	(c)	47	23.9	15.2	8.6

[a]Specimen damaged before postexposure data taken.

[b]No spectrographic data available for 30.48-centimeter stream.

[c]Test ended after 1260 seconds (ΔT = 241° F (134° K)).

TABLE II.- SUMMARY OF RESULTS FOR LOW-DENSITY SILICONE RESIN

(a) U.S. customary units

[ρ = 55 lb/ft^3; w = 3 lb/ft^2; specimen thickness = 0.66 in.]

Specimen	Stream diam. in.	$\dot{W}/A$, $\frac{lb}{ft^2\text{-sec}}$	C, percent	$\dot{q}$, Btu/ft^2-sec	H_∞, Btu/lb	τ, lb/ft^2	t_{300}, sec	E_{300}, Btu/lb	Wt. loss, percent	Thickness, in.		
										Total	Virgin	Char
38	2	16	23	193	3400	6.40	91	5860	94	0.28	(a)	(a)
39	2	16	11	118	2200	4.93	312	12280	21	.60	0.07	0.53
40	2	16	11	206	3600	6.54	102	7000	99	(a)	(a)	(a)
41	2	16	3	93	2050	3.94	311	9640	26	.73	.06	.67
42	2	16	3	132	2250	5.57	260	11450	29	.48	.04	.44
43	2	16	3	133	2250	5.57	270	11980	29	.55	.03	.52
44	2	16	3	140	2275	5.87	295	13770	13	.46	.06	.40
45	2	16	3	160	2700	6.13	236	12590	66	.28	.04	.24
46	2	16	3	195	3400	6.45	169	10940	(a)	(a)	(a)	(a)
47	2	16	3	217	3750	6.75	102	7370	(a)	.33	(a)	(a)
48	2	16	0	95	2050	4.03	315	9975	44	.60	.05	.55
49	2	16	0	175	2950	6.35	201	11715	98	.40	(a)	(a)
50	2	16	0	200	3500	6.47	150	10000	83	.48	.15	.33
51	4	4	23	101	3250	.83	356	12000	(a)	(a)	(a)	(a)
52	4	4	3	112	3400	.90	321	12000	(a)	(a)	(a)	(a)
53	6	1.8	23	66	2350	.27	356	7840	13	.66	.14	.52
54	6	1.8	11	66	2350	.27	358	7840	14	.69	.15	.54
55	6	1.8	11	66	2350	.27	310	6810	18	.68	.21	.47
56	6	1.8	3	43	1900	.20	429	6150	9	.77	.23	.54
57	6	1.8	3	66	2675	.26	426	7170	14	.75	.14	.61
58	6	1.8	3	84	3150	.30	278	7780	15	.78	.14	.64
59	6	1.8	0	66	2550	.26	364	8000	12	.70	.18	.52
60	12	.2	23	20	(b)	0	658	4380	9	.73	.21	.52
61	12	.2	11	12	(b)	0	666	2641	10	.78	.33	.45
62	12	.2	3	13	(b)	0	1005	4450	9	.83	.28	.55
63	12	.2	3	22	(b)	0	652	4820	23	.80	.08	.72
64	12	.2	3	36	(b)	0	443	5320	17	.83	.14	.69
65	12	.2	0	9	(b)	0	1072	3250	7	.82	.39	.43

[a]Specimen damaged before postexposure data taken.

[b]No spectrographic data available for 12-inch test stream.

TABLE II.- SUMMARY OF RESULTS FOR LOW-DENSITY SILICONE RESIN - Concluded

(b) SI units

[ρ = 880 kg/m^3; w = 14.7 kg/m^2; specimen thickness = 1.8 cm]

Specimen	Stream diam, cm	$\dot{W}/A$, lb/ft^2-sec	C, percent	q, Btu/ft^2-sec	H_∞, Btu/lb	τ, lb/ft^2	t_{300}, sec	E_{300}, Btu/lb	Wt. loss, percent	Thickness, in.		
										Total	Virgin	Char
38	5.08	78	23	2.19	7.88	306	91	13.6	94	7.1	(a)	(a)
39	5.08	78	11	1.34	5.10	236	312	28.5	21	15.2	1.78	13.5
40	5.08	78	11	2.34	8.35	313	102	16.2	99	(a)	(a)	(a)
41	5.08	78	3	1.05	4.76	189	311	22.4	26	18.5	1.52	17
42	5.08	78	3	1.50	5.22	267	260	26.6	29	12.2	1.02	11.2
43	5.08	78	3	1.51	5.22	267	270	27.8	29	14	.80	13.2
44	5.08	78	3	1.59	5.27	281	295	31.9	13	11.7	1.50	10.2
45	5.08	78	3	1.81	6.26	294	236	29.2	66	7.1	1.00	6.1
46	5.08	78	3	2.21	7.88	309	169	25.4	(a)	(a)	(a)	(a)
47	5.08	78	3	2.46	8.70	323	102	17.1	(a)	8.4	(a)	(a)
48	5.08	78	0	1.08	4.76	193	315	23.1	44	15.2	1.30	13.9
49	5.08	78	0	1.99	6.84	304	201	27.2	98	10.2	(a)	(a)
50	5.08	78	0	2.27	8.11	310	150	23.2	83	12.2	3.80	8.4
51	10.16	19.5	23	1.15	7.54	39.7	356	27.8	(a)	(a)	(a)	(a)
52	10.16	19.5	3	1.27	7.88	43.1	321	27.8	(a)	(a)	(a)	(a)
53	15.24	8.7	23	.75	5.45	12.9	356	18.2	13	16.8	3.60	13.2
54	15.24	8.7	11	.75	5.45	12.9	358	18.3	14	17.5	3.80	13.7
55	15.24	8.7	11	.75	5.45	12.9	310	15.8	18	17.3	5.30	12.0
56	15.24	8.7	3	.49	4.40	9.6	429	14.3	9	19.5	5.80	13.7
57	15.24	8.7	3	.75	6.20	12.4	326	16.6	14	19.0	3.60	15.4
58	15.24	8.7	3	.95	7.30	14.4	278	18.0	15	19.8	3.60	16.2
59	15.24	8.7	0	.75	5.92	12.4	364	18.6	12	17.8	4.60	13.2
60	30.48	.97	23	.23	(b)	0	658	10.2	9	18.5	5.30	13.2
61	30.48	.97	11	.14	(b)	0	666	6.1	10	19.8	8.40	11.4
62	30.48	.97	3	.15	(b)	0	1005	10.3	9	21	7.10	13.9
63	30.48	.97	3	.25	(b)	0	652	11.2	23	20.3	2.00	18.3
64	30.48	.97	3	.41	(b)	0	443	12.3	17	21	3.60	17.4
65	30.48	.97	0	.10	(b)	0	1072	7.5	7	20.8	9.90	10.9

[a]Specimen damaged before postexposure data taken.

[b]No spectrographic data available for 30.48-centimeter test stream.

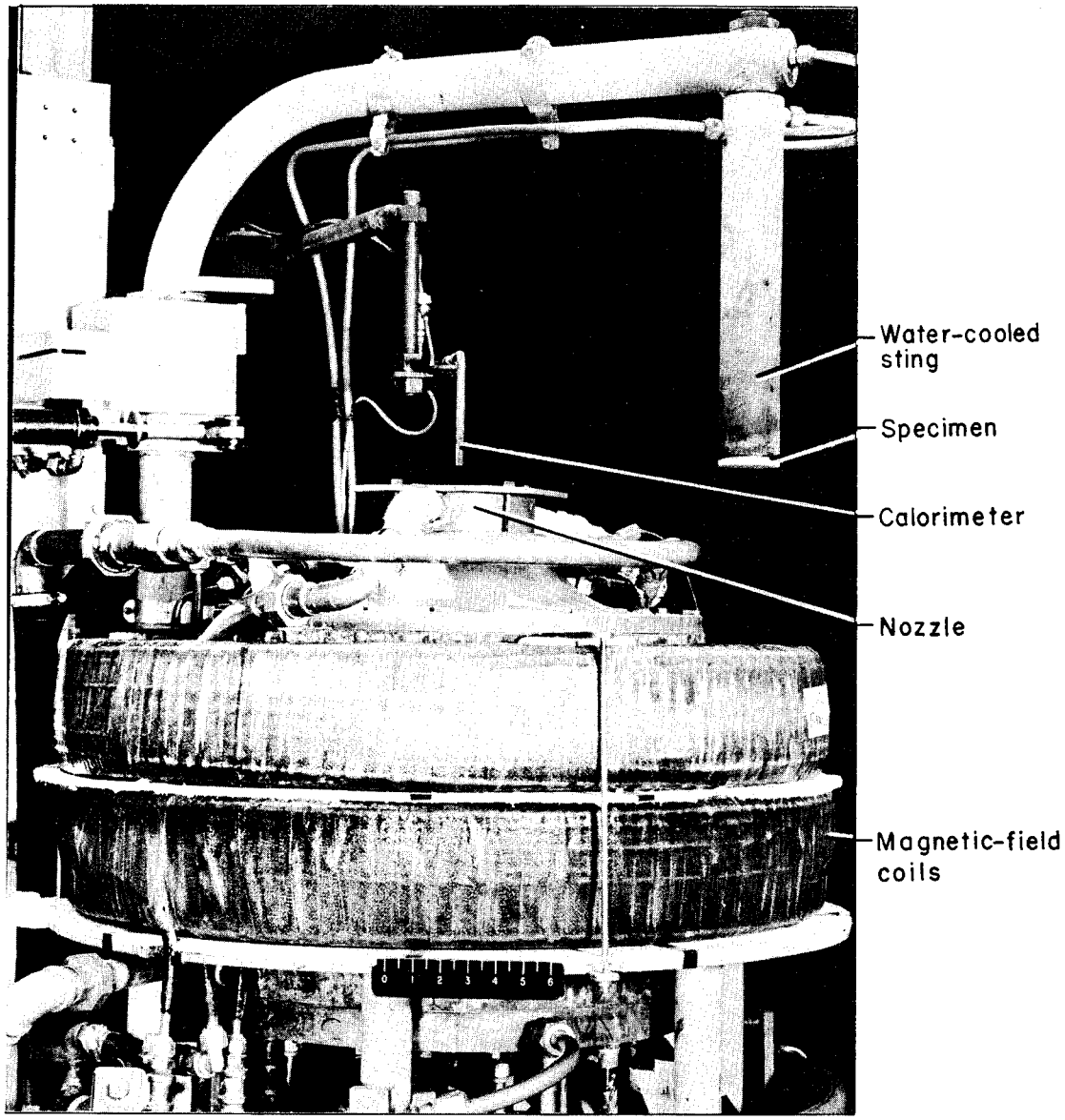

Figure 1.- The 2500-kilowatt arc jet at Langley Research Center. L-64-8315

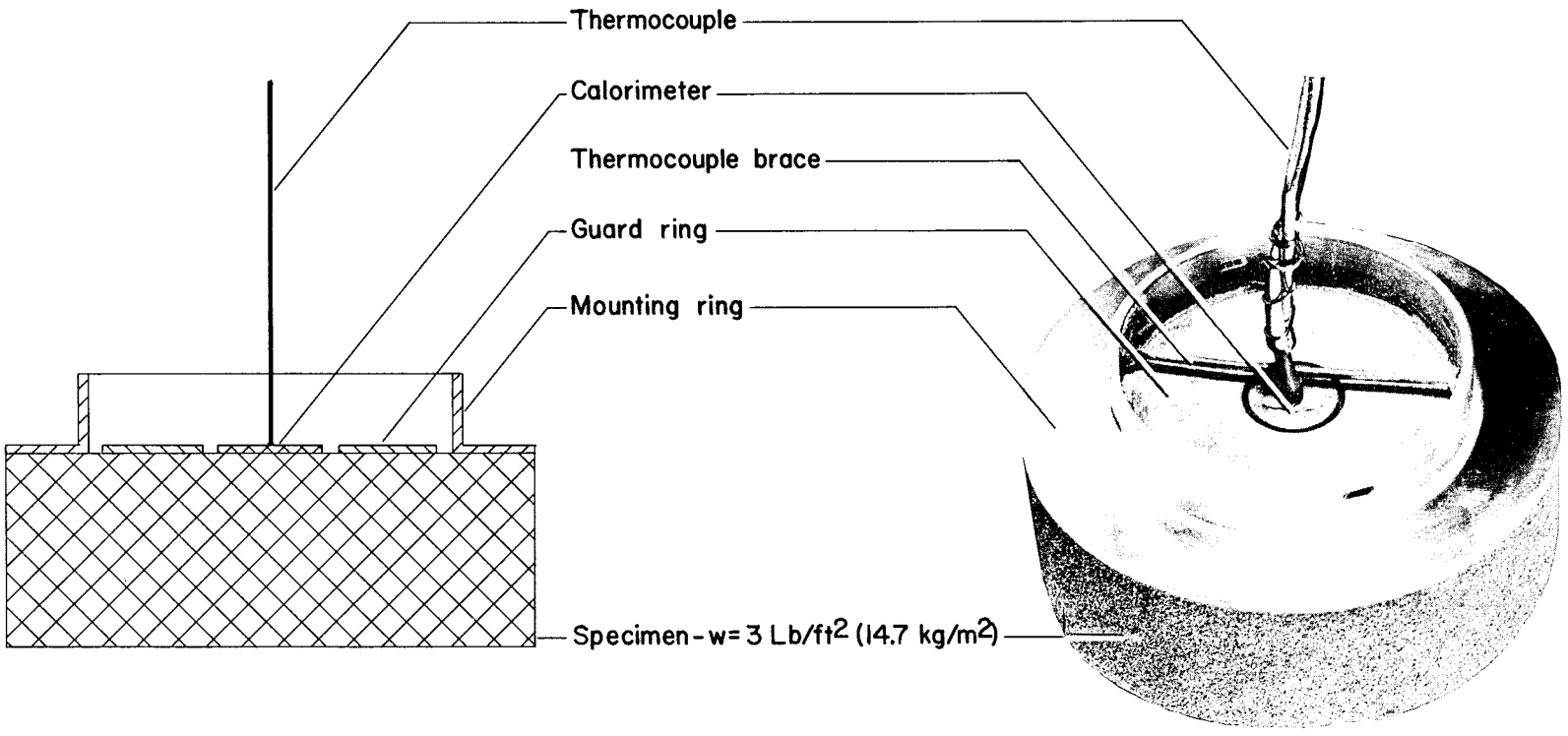

Figure 2.- Specimen mounting and instrumentation details. L-64-8316

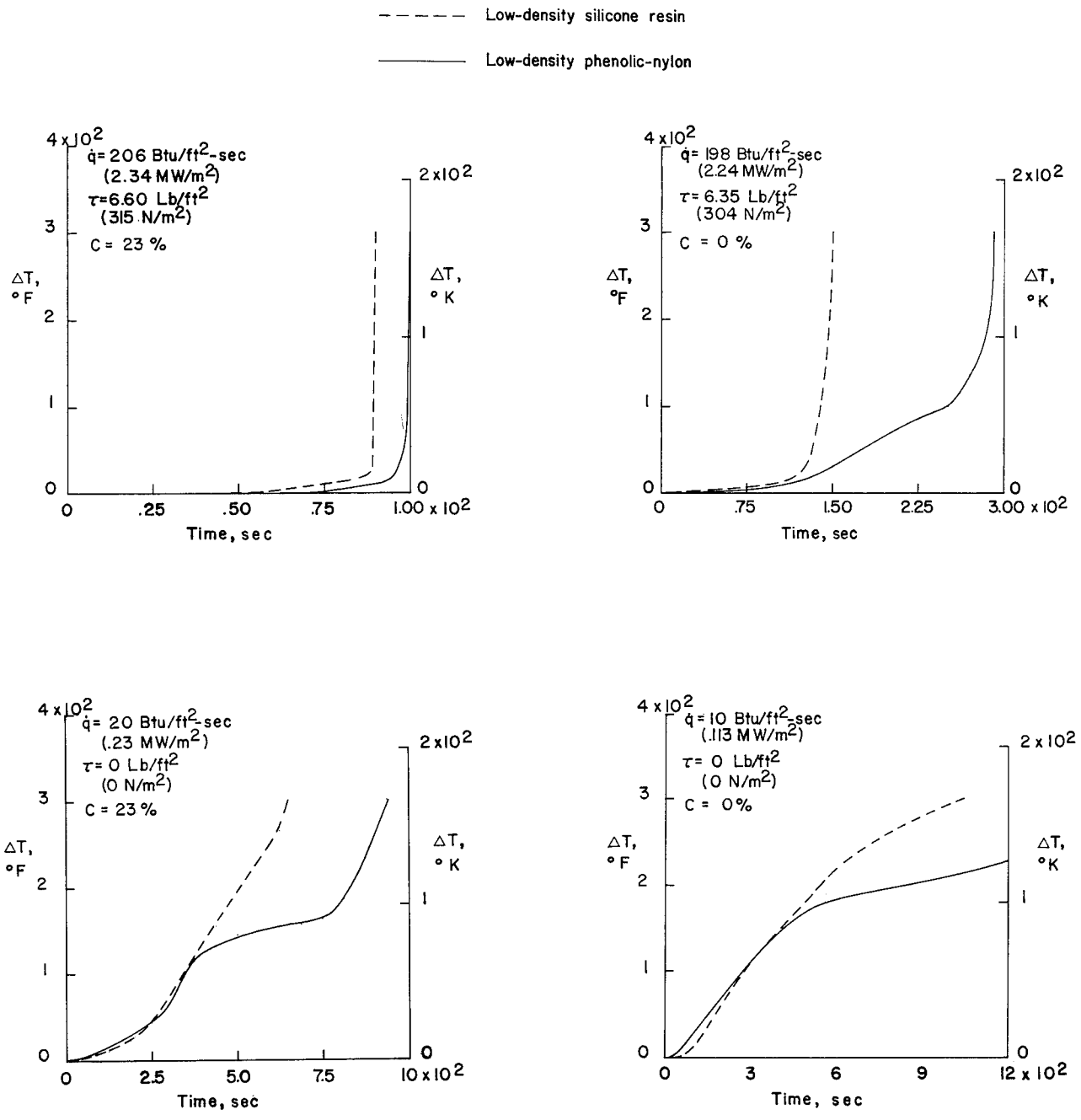

Figure 3.- Representative plots of back-surface temperature rise for low-density silicone resin and low-density phenolic-nylon.

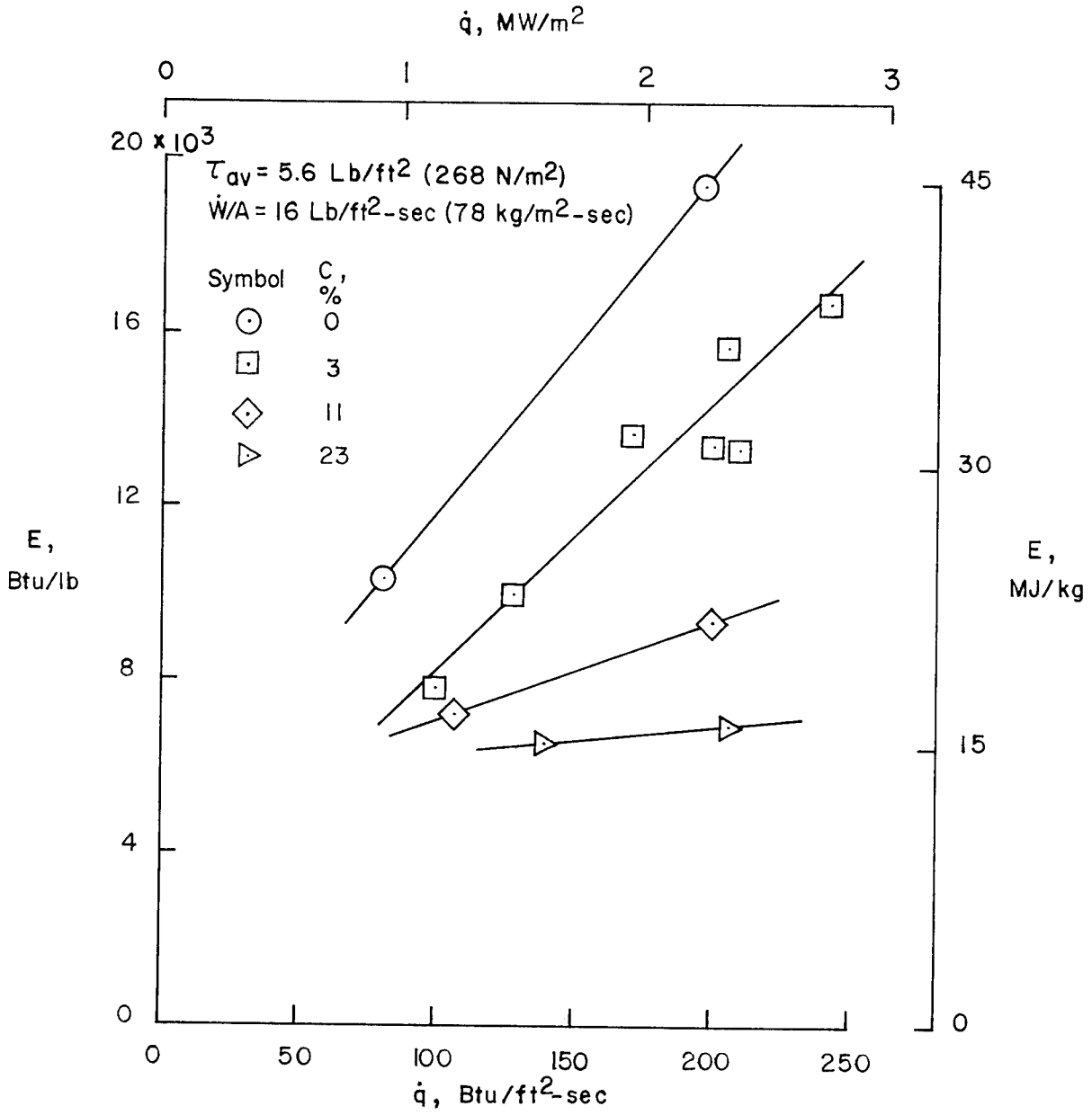

Figure 4.- Effectiveness of low-density phenolic-nylon as a function of heating rate and stream chemistry.

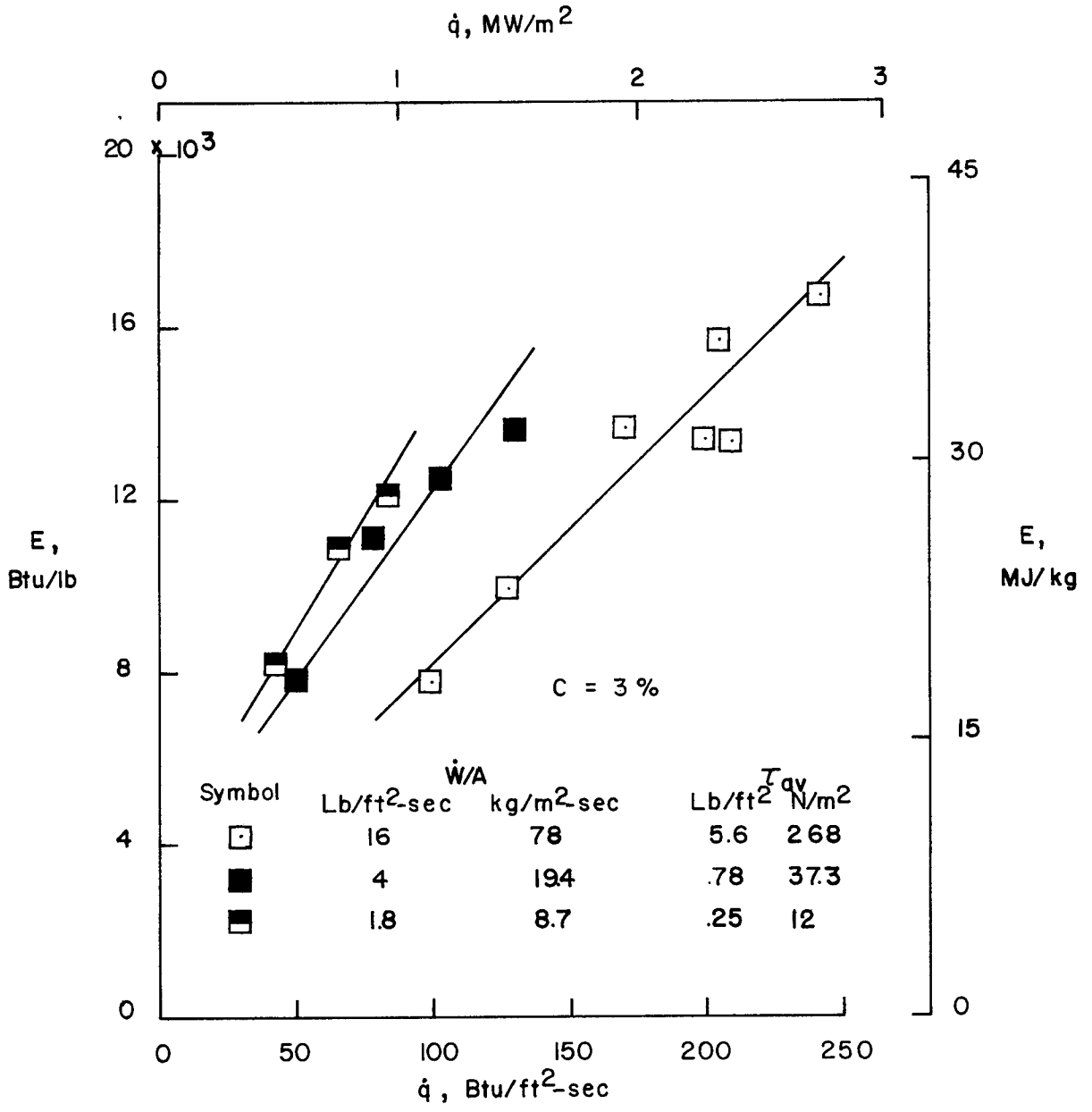

Figure 5.- Effectiveness of low-density phenolic-nylon as a function of heating rate, stream mass flow, and aerodynamic shear stress.

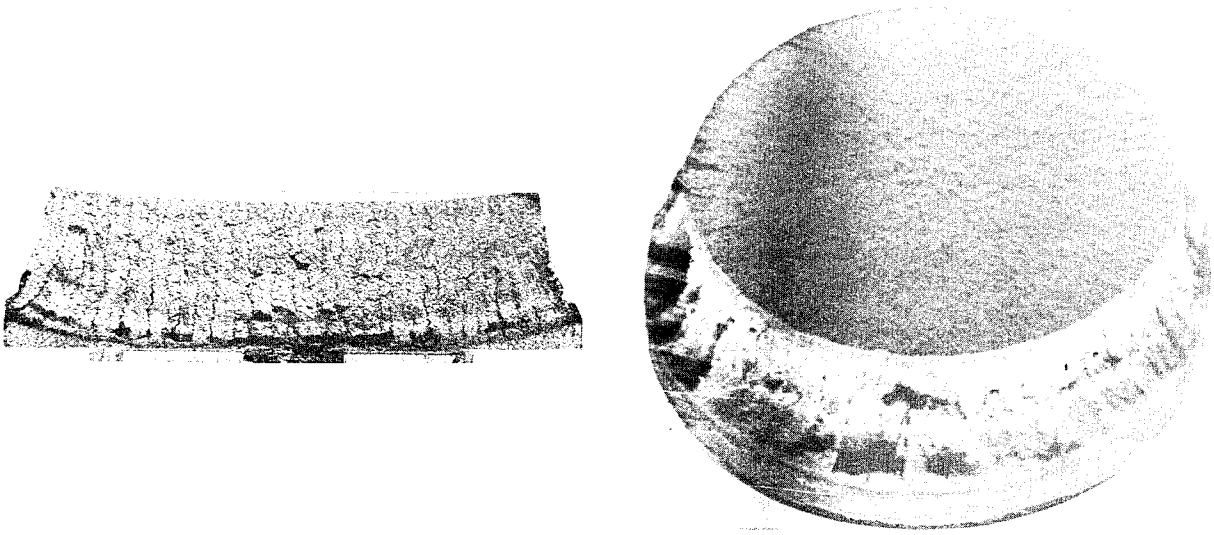

(a) Specimen 13; C = 0 percent.

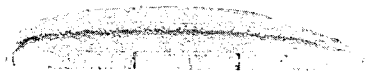

(b) Specimen 2; C = 23 percent.

L-64-8317

Figure 6.- Low-density phenolic-nylon exposed to nominal heating rate of 200 Btu/ft^2-sec (2.27 MW/m^2) with $\dot{W}/A$ = 16 lb/ft^2-sec (78 kg/m^2-sec).

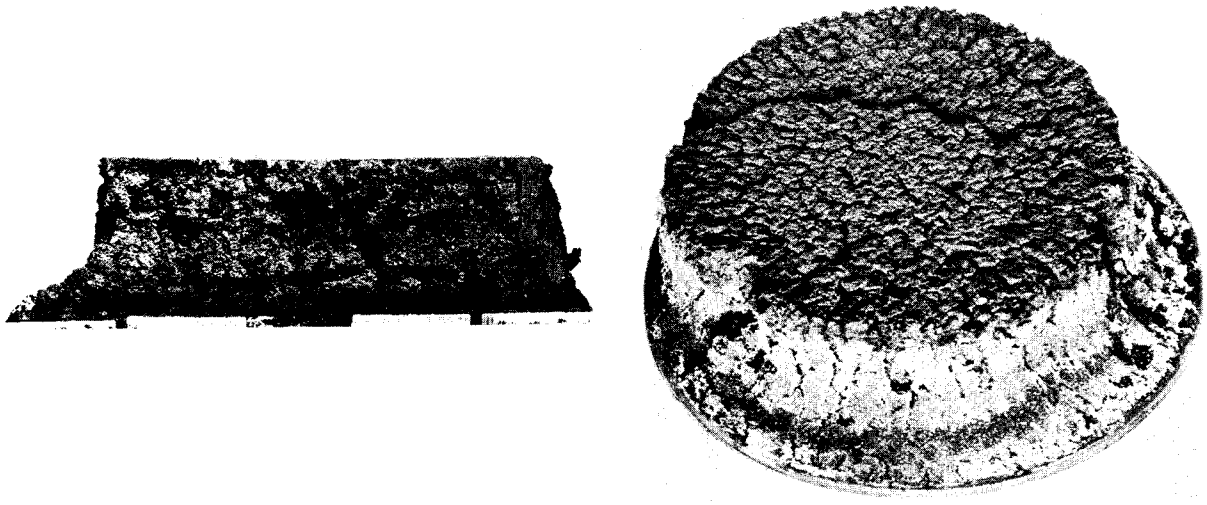

(a) Specimen 12; C = 0 percent.

(b) Specimen 5; C = 3 percent. L-64-8318

Figure 7.- Low-density phenolic-nylon exposed to nominal heating rate of 90 Btu/ft^2-sec (1.02 MW/m^2) with $\dot{W}/A$ = 16 lb/ft^2-sec (78 kg/m^2-sec).

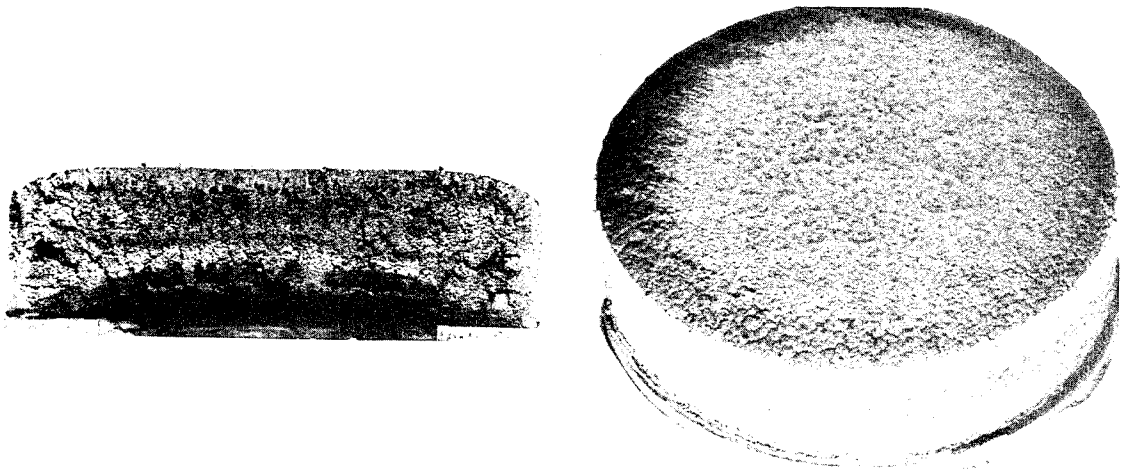

(a) Specimen 24; C = 0 percent.

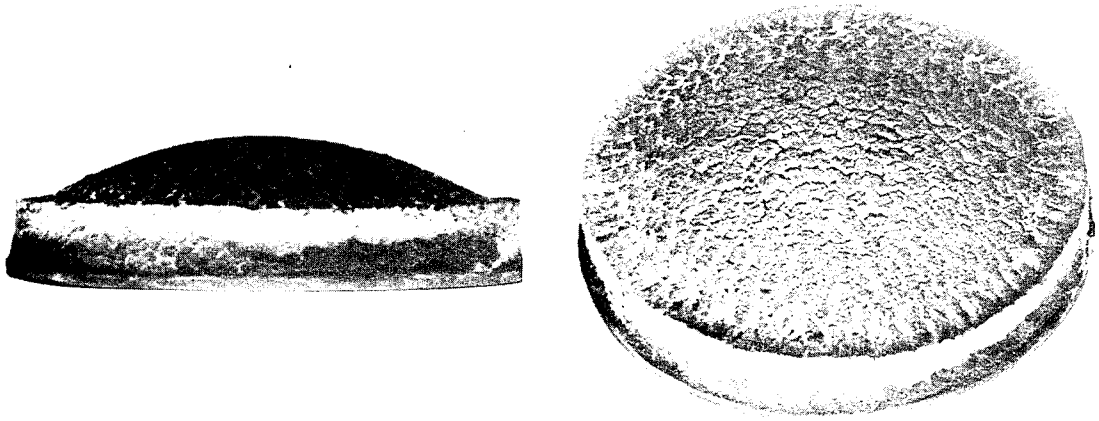

(b) Specimen 21; C = 3 percent.

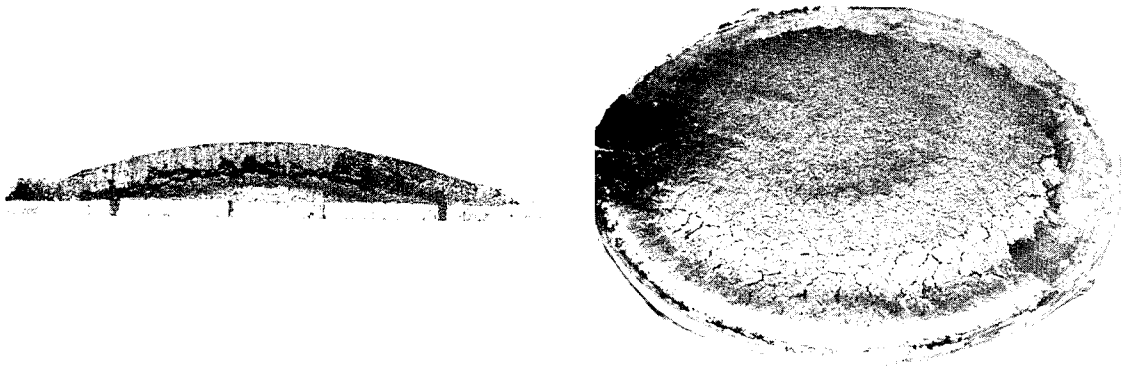

(c) Specimen 18; C = 11 percent. L-64-8319

Figure 8.- Low-density phenolic-nylon exposed to nominal heating rate of 105 Btu/ft^2-sec (1.19 MW/m^2) with $\dot{W}/A$ = 4 lb/ft^2-sec (19.4 kg/m^2-sec).

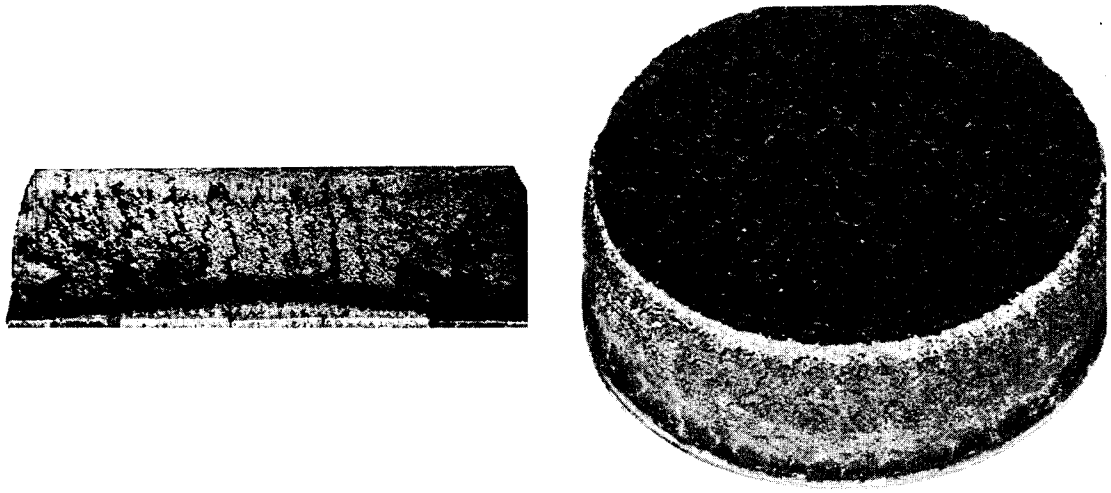

(a) Specimen 23; C = 0 percent.

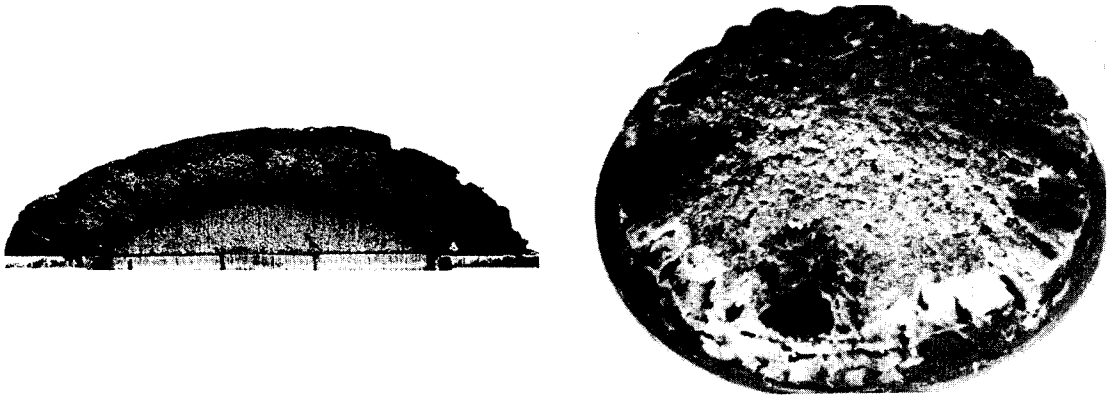

(b) Specimen 19; C = 3 percent

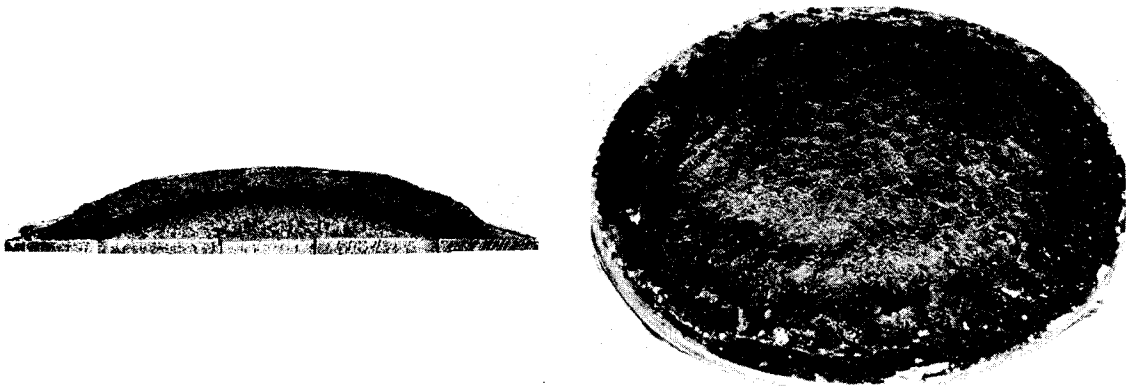

(c) Specimen 17; C = 11 percent.

L-64-8320

Figure 9.- Low-density phenolic-nylon exposed to nominal heating rate of 50 Btu/ft^2-sec (0.57 MW/m^2) with $\dot{W}/A$ = 4 lb/ft^2-sec (19.4 kg/m^2).

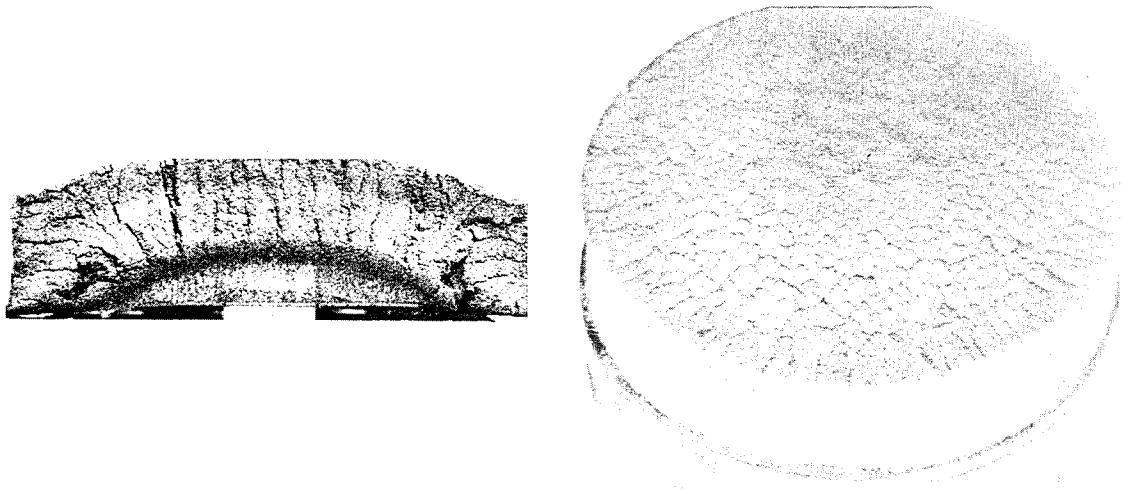

(a) Specimen 31; C = 3 percent.

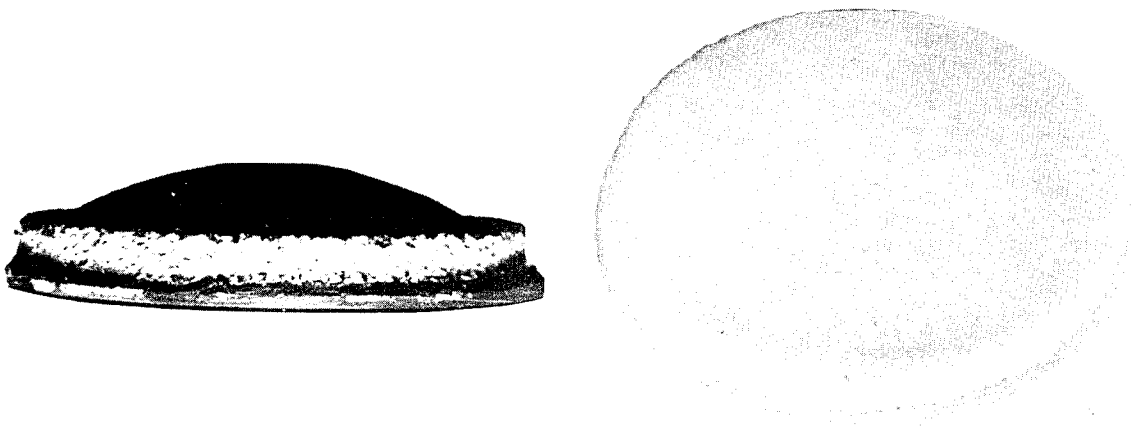

(b) Specimen 28; C = 11 percent.

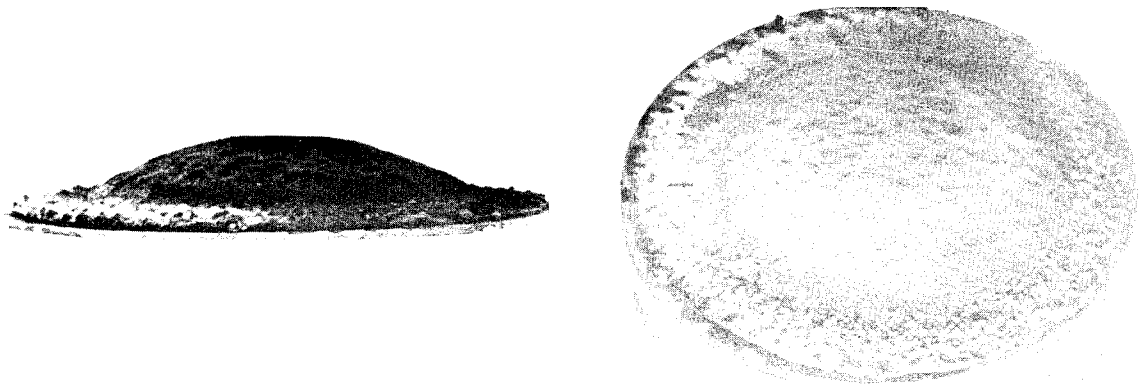

(c) Specimen 25; C = 23 percent. L-64-8321

Figure 10.- Low-density phenolic-nylon exposed to nominal heating rate of 66 Btu/ft^2-sec (0.75 MW/m^2) with $\dot{W}/A$ = 1.8 lb/ft^2-sec (8.7 kg/m^2-sec).

(a) Specimen 30; C = 3 percent.

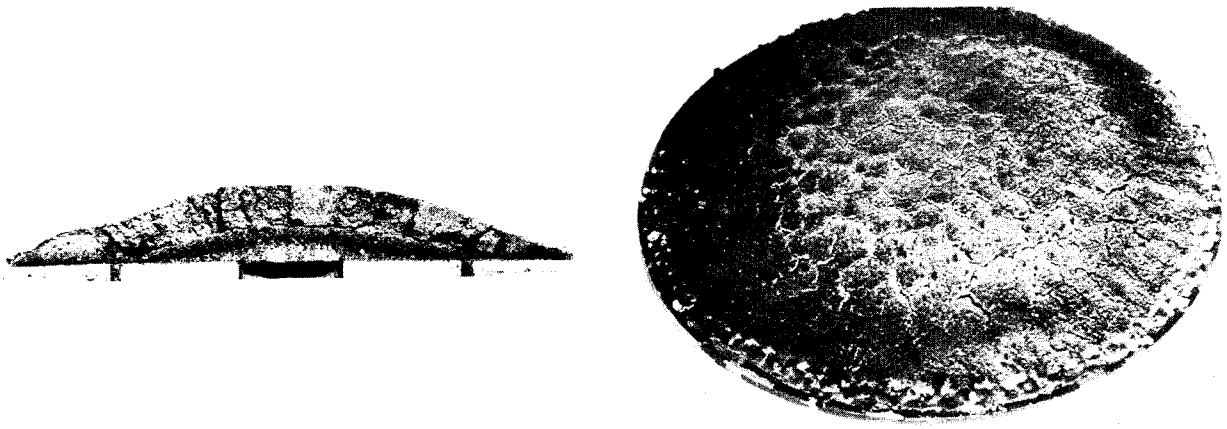

(b) Specimen 27; C = 11 percent. L-64-8322

Figure 11.- Low-density phenolic-nylon exposed to nominal heating rate of 42 Btu/ft^2-sec (0.48 MW/m^2) with $\dot{W}/A$ = 1.8 lb/ft^2-sec (8.7 kg/m^2-sec).

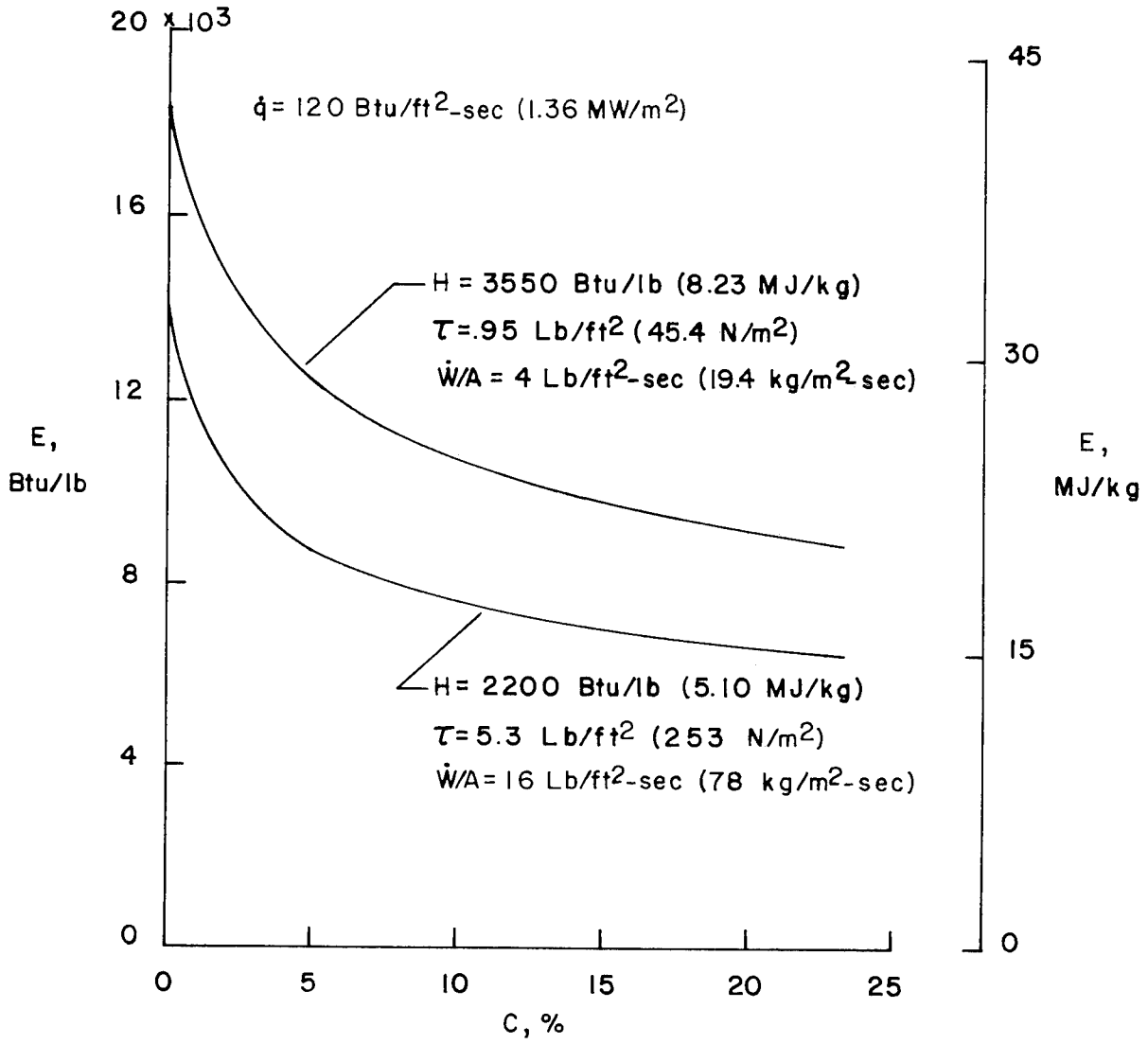

Figure 12.- Effectiveness of low-density phenolic-nylon as a function of stream chemistry, enthalpy, mass flow, and aerodynamic shear stress.

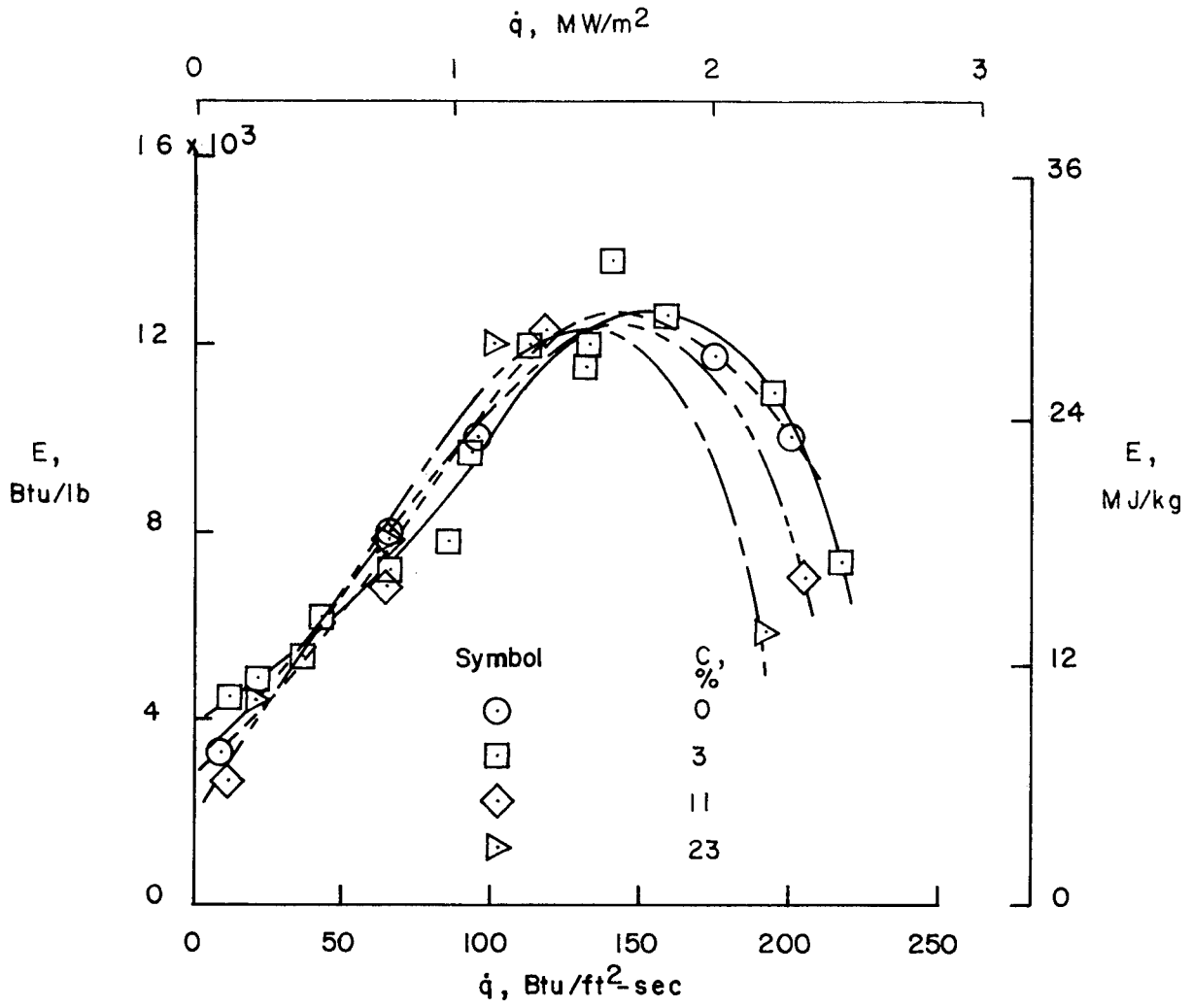

Figure 13.- Effectiveness of low-density silicone resin as a function of heating rate and stream chemistry.

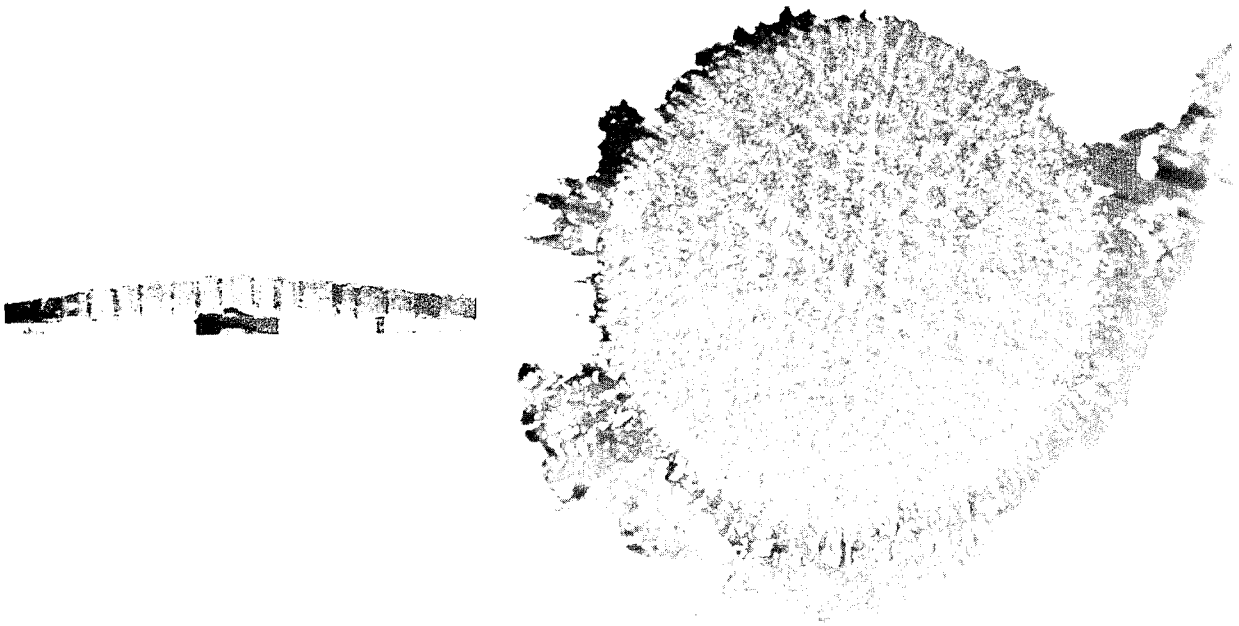

L-64-8323

Figure 14.- Low-density silicone resin exposed to a heating rate of 160 Btu/ft^2-sec (1.82 MW/m^2) with $\dot{W}/A$ = 16 lb/ft^2-sec (78 kg/m^2-sec). Specimen 45; C = 3 percent.

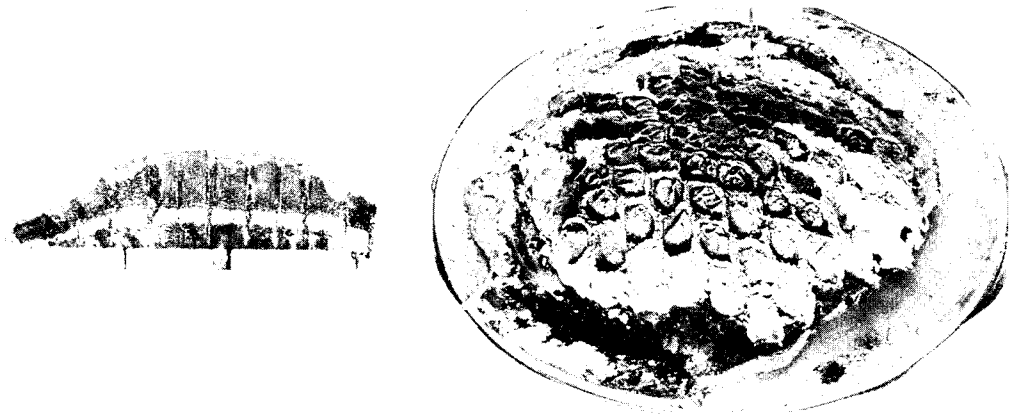

L-64-8324

Figure 15.- Low-density silicone resin exposed to a heating rate of 200 Btu/ft^2-sec (2.27 MW/m^2) with $\dot{W}/A$ = 16 lb/ft^2-sec (78 kg/m^2-sec). Specimen 50; C = 0 percent.

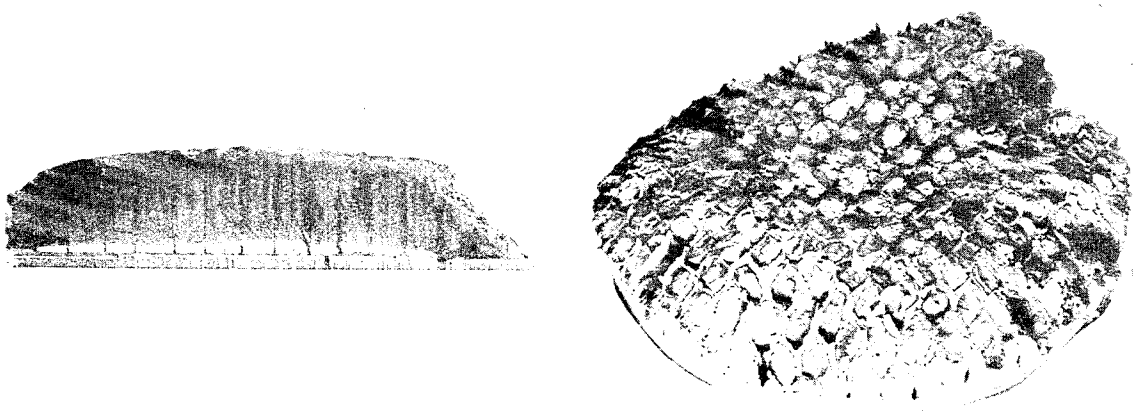

(a) Specimen 48; C = 0 percent.

(b) Specimen 41; C = 3 percent.

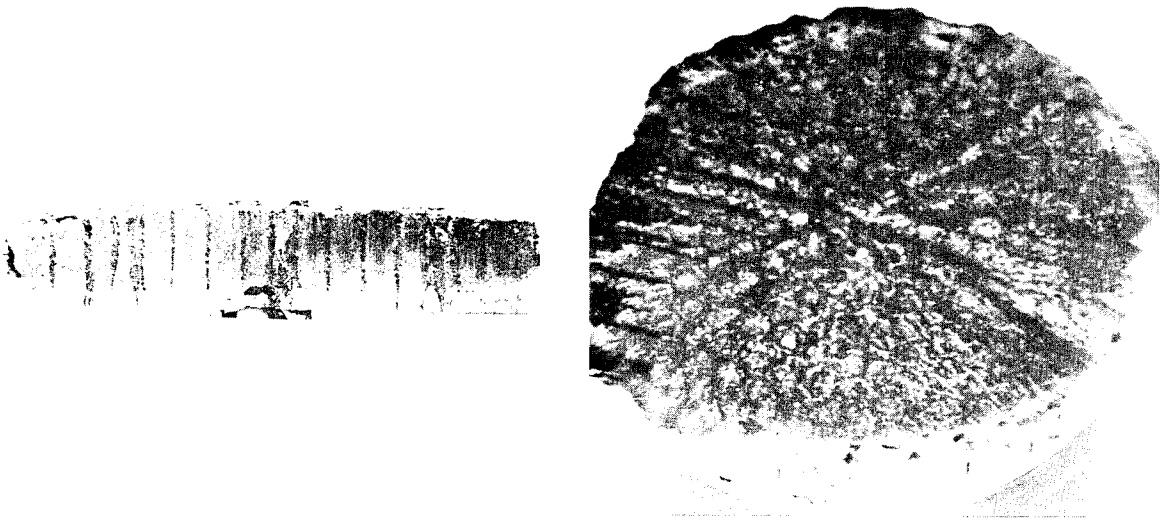

(c) Specimen 39; C = 11 percent. L-64-8325

Figure 16.- Low-density silicone resin exposed to nominal heating rate of 100 Btu/ft^2-sec (1.13 MW/m^2) with $\dot{W}/A$ = 16 lb/ft^2-sec (78 kg/m^2-sec).

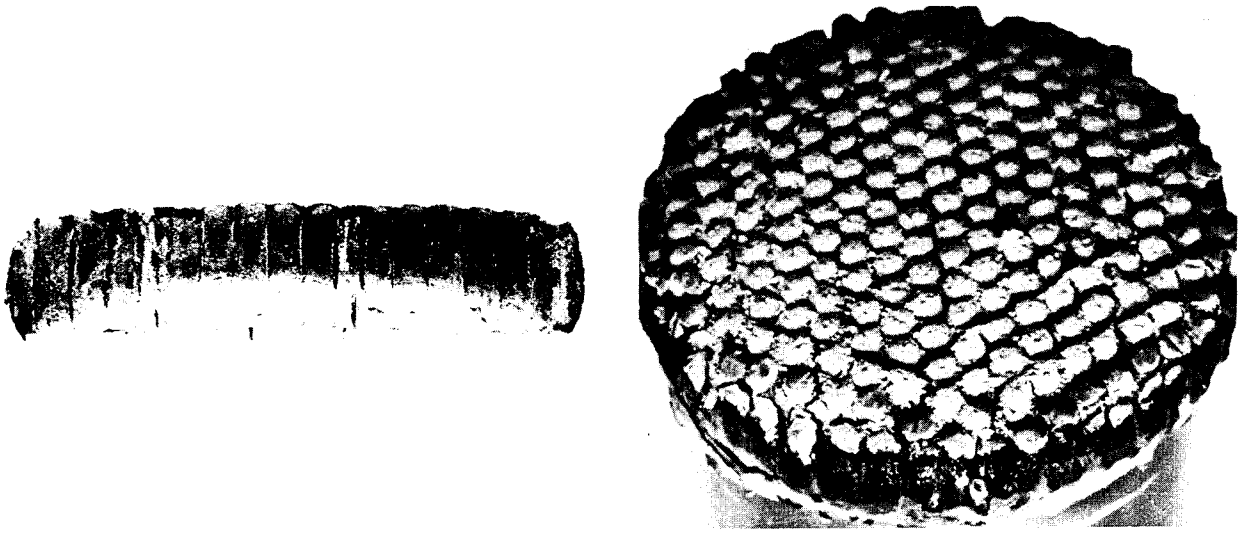

(a) Specimen 59; C = 0 percent.

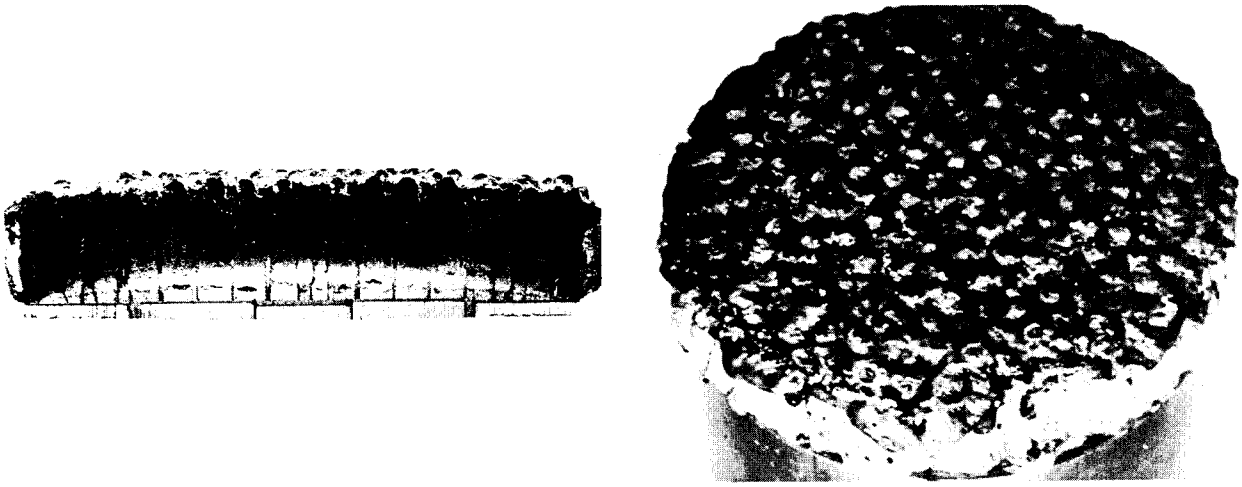

(b) Specimen 53; C = 23 percent. L-64-8326

Figure 17.- Low-density silicone resin exposed to nominal heating rate of 66 Btu/ft^2-sec (0.75 MW/m^2) with $\dot{W}/A$ = 1.8 lb/ft^2-sec (8.7 kg/m^2-sec).

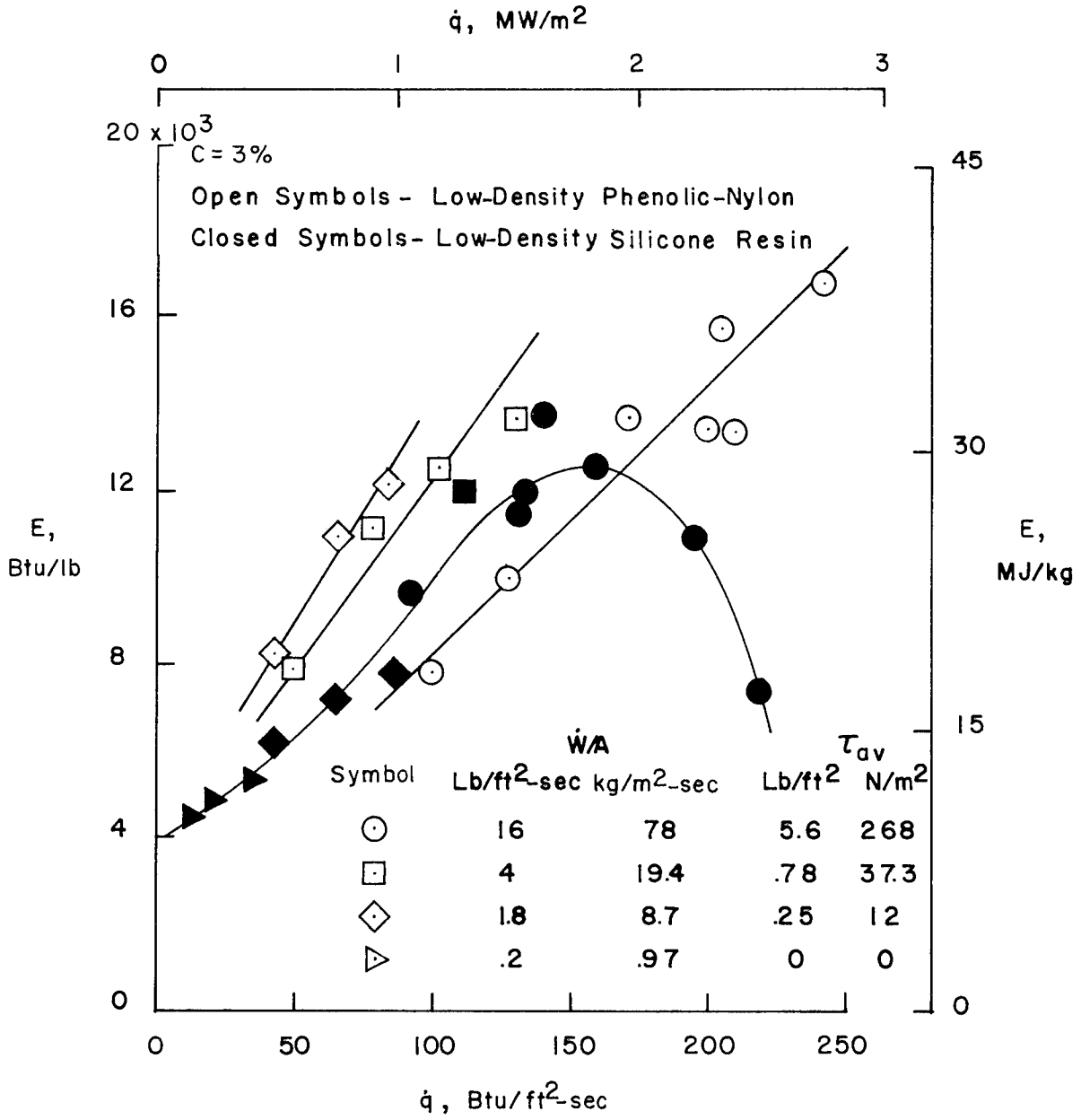

Figure 18.- Effectiveness of low-density phenolic-nylon and silicone resin as a function of heating rate, stream mass flow, and aerodynamic shear stress.

NASA-Langley, 1965 L-3411